



THESIS APPROVAL
GRADUATE SCHOOL, KASETSART UNIVERSITY

Master of Engineering (Chemical Engineering)
DEGREE

Chemical Engineering
FIELD

Chemical Engineering
DEPARTMENT

TITLE: Modification of Pore Size of SBA-15 Mesoporous Silica Produced from
Rice Husk Ash

NAME: Ms. Suchada Issaraporn

THIS THESIS HAS BEEN ACCEPTED BY

Metta Chareonpanich

THESIS ADVISOR

(Associate Professor Metta Chareonpanich, D.Eng.)

Paisan Kongkachuichay

COMMITTEE MEMBER

(Associate Professor Paisan Kongkachuichay, Ph.D.)

Chart Chiemchaisri

COMMITTEE MEMBER

(Associate Professor Chart Chiemchaisri, D.Eng.)

Thumrongrut Mungcharoen

DEPARTMENT HEAD

(Assistant Professor Thumrongrut Mungcharoen, Ph.D.)

APPROVED BY THE GRADUATE SCHOOL ON 31/08/2006

Vinai Artkongharn

DEAN

(Associate Professor Vinai Artkongharn, M.A.)

THESIS

MODIFICATION OF PORE SIZE OF SBA-15 MESOPOROUS SILICA PRODUCED FROM RICE HUSK ASH

SUCHADA ISSARAPORN

**A Thesis Submitted in Partial Fulfillment of
the Requirements for the Degree of
Master of Engineering (Chemical Engineering)
Graduate School, Kasetsart University
2006**

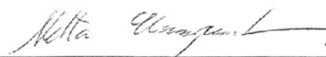
ISBN 974-16-2625-8

Suchada Issaraporn 2006: Modification of Pore Size of SBA-15 Mesoporous Silica Produced from Rice Husk Ash. Master of Engineering (Chemical Engineering), Major Field: Chemical Engineering, Department of Chemical Engineering. Thesis Advisor: Associate Professor Metta Chareonpanich, D.Eng. 97 pages.
ISBN 974-16-2625-8

In this research, the pore diameter of SBA-15 mesoporous silica synthesized from rice husk ash has been modified by using swelling agents such as 1,3,5-trimethylbenzene (TMB), 2,3,4-trimethylpentane (TMP), tetrahexylammonium bromide (THB) and N,N-dimethyldecylamine (DMD) and operating conditions. The DOE study of the effect of operating conditions including hydrolysis-condensation temperature, hydrothermal treatment temperature, amount of hydrochloric acid and swelling agents on the surface area, pore size and pore size distribution of synthesized materials were investigated. It was found that hydrolysis-condensation temperature and hydrothermal treatment temperature have great effect for the control of the pore size and pore size distribution in the range of 2-50 nm. The hydrolysis-condensation temperature of 35°C and hydrothermal treatment temperature of 110°C are the optimum synthesis temperatures. SBA-15 obtained at this condition has pore diameter of 7.7 nm, high surface area of 885 m²/g, total pore volume of 0.31 cm³/g and well-ordered hexagonal structure. The effect of swelling agents were investigated for expanding the SBA-15 pore diameter. The swelling effect can be arranged in order as follows: TMB > TMP > THB ≈ DMD. Maximum pore diameter of SBA-15 is approximately 31 nm when TMB was used as the swelling agent. The formation mechanism of SBA-15 mesoporous silica with the addition of various types of swelling agents were proposed.

SUCHADA ISSARAPORN

Student's signature



Thesis Adviser's signature

18 / 08 / 2006

ACKNOWLEDGMENTS

First of all, I would like to thank and express my respect to my advisor, Associate Professor Metta Chareonpanich, for giving me not only a chance to work in her group, but also the permanent positive influences by her personal characteristics and enthusiastic working way. I am so sincerely grateful to my co-advisor, Associate Professor Paisarn Kongkachuichay, for his advice and invaluable ideas. I am very thankful to Associate Professor Chart Chiemchaisri and Associate Professor Pakawadee Sutthivaiyakit for their kindly giving the time to comment my thesis.

I am also grateful to the administrative help received from the Department of Chemical Engineering. I would like to extend my thanks to all my friends at MTC group for their care and help in so many ways. Their friendships are of the greatest importance to me.

Finally, I am deeply indebted to my parents for giving me a nice family and always supporting me in everything I do.

Financial supports from the Postgraduate Education and Research Programs in Petroleum and Petrochemical Technology funded by ADB-MUA, the Commission on Higher Education and the Thailand Research Fund (RMU 4880016), the Thailand Research Fund (Senior-TRF, Professor Jumras Limtrakul) and the Kasetsart University Research and Development Institute (KURDI) are gratefully acknowledged.

Suchada Issaraporn
June 2006

TABLE OF CONTENTS

	Page
TABLE OF CONTENTS	i
LIST OF TABLES	ii
LIST OF FIGURES	iii
INTRODUCTION	1
Objectives of Research	2
Scope of Research	2
LITERATURE REVIEWS	3
Rice husk ash	3
Mesoporous materials	4
SBA-15 mesoporous silica	18
MATERIALS AND METHODS	25
Materials	25
Methods	26
RESULTS AND DISCUSSION	30
Rice husk ash	30
Design of experiments (DOE)	31
The optimum synthesis condition	35
Modification of pore size of SBA-15 mesoporous silica	48
Formation mechanism of SBA-15 mesoporous silica	53
CONCLUSIONS	61
LITERATURE CITED	62
APPENDIX	69
CURRICULUM VITAE	97

LIST OF TABLES

Table		Page
1	The chemical compositions of rice husk ash	3
2	Physical properties of various mesoporous silica materials	5
3	Various mesoporous silica based on 2D hexagonal (<i>P6mm</i>)	11
4	Details of experimental design conditions	29
5	Physical properties of various types of swelling agents	48
Appendix Table		
A1	Boundary values of each factor for synthesizing SBA-15 mesoporous silica	72
A2	Effect of each factor on surface area and pore size of SBA-15 mesoporous silica	73
A3	Contrast value in Equation (A1) for the 2 ⁴ design	74
A4	Contrast and factor effect values for 2 ⁴ factorial design on pore size and surface area of SBA-15 mesoporous silica	75
A5	The result of % normal probability on pore size of SBA-15 mesoporous silica	76
A6	The result of % normal probability on surface area of SBA-15 mesoporous silica	78
A7	Synthesis temperature condition	80
B1	Effect of synthesis temperature conditions on surface area, pore volume and pore size of SBA-15 products	91
B2	Effect of swelling agents on SBA-15 properties	92

LIST OF FIGURES

Figure		Page
1	The sol-gel process for the silica network preparation	7
2	Micellization of surfactant in aqueous solution	8
3	Block copolymer templates used in mesoporous materials	9
4	The liquid crystal templating mechanism for the formation of MCM-41: (1) liquid-crystal-phase-initiated and (2) silicate-anion-initiated	12
5	(a) The procedure of a mesoporous oxide network synthesis from the solution and (b) the main relationships of mesostructured hybrid	13
6	The expansion of surfactant micelle with 1,3,5-trimethyl benzene (TMB) as swelling agent	15
7	Nitrogen adsorption isotherm of SBA-15 mesoporous silica materials	20
8	SEM image of SBA-15 mesoporous silica	20
9	TEM image of calcined hexagonal SBA-15 mesoporous silicas	21
10	XRD pattern of (A) as synthesized and (B) calcined SBA-15 mesoporous silica	22
11	XRD pattern of rice husk ash	30
12	Pore size distribution of rice husk ash	31
13	Normal probability plot of the effects for the 2^4 factorial on the pore size	33
14	Normal probability plot of the effects for the 2^4 factorial on the surface area	34
15	Pore size distribution of SBA-15 mesoporous silica obtained from various hydrolysis-condensation temperatures at the hydrothermal treatment temperature of 90°C	36

LIST OF FIGURES (cont'd)

Figure		Page
16	Pore size distribution of SBA-15 mesoporous silica obtained from various hydrolysis-condensation temperatures at the hydrothermal treatment temperature of 100°C	36
17	Pore size distribution of SBA-15 mesoporous silica obtained from various hydrolysis-condensation temperatures at the hydrothermal treatment temperature of 110°C	37
18	Pore size distribution of SBA-15 mesoporous silica obtained from various hydrolysis-condensation temperatures at the hydrothermal treatment temperature of 120°C	37
19	Effect of hydrothermal treatment temperatures and hydrolysis-condensation temperatures on the surface area of SBA-15 mesoporous silica	39
20	Effect of hydrothermal treatment temperatures and hydrolysis-condensation temperatures on the pore volume of SBA-15 mesoporous silica	39
21	Effect of hydrothermal treatment temperatures and hydrolysis-condensation temperatures on the micropore volume of SBA-15 mesoporous silica	40
22	Effect of hydrothermal treatment temperatures and hydrolysis-condensation temperatures on the pore size of SBA-15 mesoporous silica	40
23	Small-angle X-ray scattering patterns of SBA-15 mesoporous silica obtained from the hydrolysis-condensation temperature at (a) 30°C (b) 35°C and (C) 40°C at the hydrothermal treatment temperature of 110°C	42

LIST OF FIGURES (cont'd)

Figure		Page
24	TEM image of SBA-15 mesoporous silica obtained from the hydrolysis-condensation temperature of 30°C and the hydrothermal treatment temperature of 110°C	43
25	TEM image of (a) perpendicular c-axis and (b) perpendicular a-axis of hexagonal lattice SBA-15 mesoporous silica obtained from the hydrolysis-condensation temperature of 35°C and the hydrothermal treatment temperature of 110°C	44
26	TEM image of SBA-15 mesoporous silica obtained from the hydrolysis-condensation temperature of 40°C and the hydrothermal treatment temperature of 110°C	45
27	SEM image of SBA-15 mesoporous silica obtained from the hydrolysis-condensation temperature of 30°C and the hydrothermal treatment temperature of 110°C	46
28	SEM image of SBA-15 mesoporous silica obtained from the hydrolysis-condensation temperature of 35°C and the hydrothermal treatment temperature of 110°C	46
29	SEM image of SBA-15 mesoporous silica obtained from the hydrolysis-condensation temperature of 40°C and the hydrothermal treatment temperature of 110°C	47
30	Effects of 1,3,5-trimethylbenzene (TMB) on pore diameter and surface area of SBA-15 mesoporous silica	49
31	Effects of 2,3,4-trimethylpentane (TMP) on pore diameter and surface area of SBA-15 mesoporous silica	50
32	Effects of tetrahexylammonium bromide (THB) on pore diameter and surface area of SBA-15 mesoporous silica	51
33	Effects of N, N-dimethyldecylamine (DMD) on pore diameter and surface area of SBA-15 mesoporous silica	52

LIST OF FIGURES (cont'd)

Figure		Page
34	X-ray diffraction patterns of SBA-15 mesoporous silicas prepared without and with using swelling agents	53
35	The formation mechanism of SBA-15 with swelling agent	55
36	The structures and schematic drawings of (a) 1,3,5-trimethylbenzene (TMB) and (b) 2,3,4-trimethylpentane (TMP)	56
37	The expansion of micelle with 1,3,5-trimethylbenzene (TMB) as swelling agent	57
38	The expansion of micelle with 2,3,4-trimethylpentane (TMP) as swelling agent	57
39	The structures and schematic drawings of (a) tetrahexylammonium bromide (THB) and (b) N, N-dimethyldecylamine (DMD)	58
40	Shrinking micelle with tetrahexylammonium bromide (THB) as swelling agent	59
41	Shrinking of micelle with N,N-dimethyldecylamine (DMD) as swelling agent	60
Appendix Figure		
A1	The relation of % normal probability and factor effect on pore size for synthesizing SBA-15 mesoporous silica	77
A2	The relation of % normal probability and factor effect on surface area for synthesizing SBA-15 mesoporous silica	79
B1	Sorption isotherm of SBA-15 product at hydrolysis-condensation temperature of 30°C and hydrothermal treatment temperature of 90°C	82

LIST OF FIGURES (cont'd)

Appendix Figure		Page
B2	Sorption isotherm of SBA-15 product at hydrolysis-condensation temperature of 30°C and hydrothermal treatment temperature of 100°C	83
B3	Sorption isotherm of SBA-15 product at hydrolysis-condensation temperature of 30°C and hydrothermal treatment temperature of 110°C	83
B4	Sorption isotherm of SBA-15 product at hydrolysis-condensation temperature of 30°C and hydrothermal treatment temperature of 120°C	84
B5	Sorption isotherm of SBA-15 product at hydrolysis-condensation temperature of 35°C and hydrothermal treatment temperature of 90°C	84
B6	Sorption isotherm of SBA-15 product at hydrolysis-condensation temperature of 35°C and hydrothermal treatment temperature of 100°C	85
B7	Sorption isotherm of SBA-15 product at hydrolysis-condensation temperature of 35°C and hydrothermal treatment temperature of 110°C	85
B8	Sorption isotherm of SBA-15 product at hydrolysis-condensation temperature of 35°C and hydrothermal treatment temperature of 120°C	86
B9	Sorption isotherm of SBA-15 product at hydrolysis-condensation temperature of 40°C and hydrothermal treatment temperature of 90°C	86
B10	Sorption isotherm of SBA-15 product at hydrolysis-condensation temperature of 40°C and hydrothermal treatment temperature of 100°C	87

LIST OF FIGURES (cont'd)

Appendix Figure		Page
B11	Sorption isotherm of SBA-15 product at hydrolysis-condensation temperature of 40°C and hydrothermal treatment temperature of 110°C	87
B12	Sorption isotherm of SBA-15 product at hydrolysis-condensation temperature of 40°C and hydrothermal treatment temperature of 120°C	88
B13	Sorption isotherm of SBA-15 product at hydrolysis-condensation temperature of 50°C and hydrothermal treatment temperature of 90°C	88
B14	Sorption isotherm of SBA-15 product at hydrolysis-condensation temperature of 50°C and hydrothermal treatment temperature of 100°C	89
B15	Sorption isotherm of SBA-15 product at hydrolysis-condensation temperature of 50°C and hydrothermal treatment temperature of 110°C	89
B16	Sorption isotherm of SBA-15 product at hydrolysis-condensation temperature of 50°C and hydrothermal treatment temperature of 120°C	90
C1	TEM image of SBA-15 mesoporous silica obtained from the hydrolysis-condensation temperature of 30°C and hydrothermal treatment temperature of 110°C	94
C2	TEM image of SBA-15 mesoporous silica obtained from the hydrolysis-condensation temperature of 35°C and hydrothermal treatment temperature of 110°C	94
C3	TEM image of SBA-15 mesoporous silica obtained from the hydrolysis-condensation temperature of 40°C and hydrothermal treatment temperature of 110°C	95

LIST OF FIGURES (cont'd)

Appendix Figure		Page
C4	TEM image of SBA-15 mesoporous silica obtained from the hydrolysis-condensation temperature of 35°C and hydrothermal treatment temperature of 90°C	95
C5	TEM image of SBA-15 mesoporous silica obtained from the hydrolysis-condensation temperature of 35°C and hydrothermal treatment temperature of 100°C	96

MODIFICATION OF PORE SIZE OF SBA-15 MESOPOROUS SILICA PRODUCED FROM RICE HUSK ASH

INTRODUCTION

Nowadays demands of transportation fuels such as gasoline and diesel oil are gradually increased all over the world. Since 2000, the requirement for amount of gasoline use and productions in Thailand have been arised to 4,022 and 5,046 million liters respectively (Department of Energy Business, 2005). Many researchers have attempted to develop the technology for gas-to-liquid (GTL) production process of which methane in the natural gas was focused as the source for hydrocarbons synthesis. In particular, diesel fuel might be produced via GTL process through the Fischer-Tropsch synthesis (synthesis of hydrocarbons from carbon monoxide and hydrogen).

The Fischer-Tropsch synthesis were catalyzed by supported metal catalysts such as Fe, Co and Ru that are promising catalysts which have shown high activities (Vannice *et al.*, 1977). Similarly, the methane reforming with carbon dioxide was also catalyzed by supported metal catalysts such as Ni, Fe, Co, Pt and Pd. In order to achieve a high density of surface active sites of metal, the porous supports such as silica (SiO₂) and alumina (Al₂O₃) are most frequently used as catalyst supports.

Recently, SBA-15 mesoporous silica was discovered by Zhao *et al.* (1998). This SBA-15 posses of periodic mesopore, high surface area (600-1,000 m²/g), narrow pore size distribution, large pore volume (1-2 cm³/g) and high thermal stability. The pore diameter of SBA-15 can be controlled in the range of 2-30 nm by the modification using various surfactants, some additives and different synthetic conditions (Zhao *et al.*, 2000).

In the present, SBA-15 mesoporous molecular sieves become more popular because the pore size is possible to be controlled. It is essential in the industrial

catalytic applications that the support selectivity and reactivity can be manipulated. A large diameter of catalyst pores also lead to higher C_{5+} selectivity (Khodakov *et al.*, 2001). On the other hands, small pore diameters lead to the lower Fischer-Tropsch reaction rates and higher methane selectivity (Khodakov *et al.*, 2001; Wang *et al.*, 2001; Panpranot *et al.*, 2002; Ohtsuka *et al.*, 2004).

In this research, SBA-15 mesoporous silica synthesized from rice husk ash was modified in order to precisely control the pore size and the pore size distribution. These SBA-15s will be applied as the catalyst support for the diesel fuel synthesis via Fischer-Tropsch reaction.

Objectives of Research

1. To synthesize SBA-15 mesoporous silica from rice husk ash.
2. To precisely control the pore size of SBA-15 by controlling operating conditions in hydrolysis-condensation stage and hydrothermal treatment stage, and using swelling agent including 1,3,5-trimethylbenzene (TMB), 2,3,4-trimethylpentane (TMP), tetrahexylammonium bromide (THB) and N, N-dimethyldecylamine (DMD).
3. To propose formation mechanisms of SBA-15 mesoporous silica obtained from synthesis process using various structure of swelling agents.

Scope of Research

In this research, the pore size and pore size distribution of SBA-15 mesoporous silica synthesized from rice husk ash were controlled by using various types and amounts of swelling agents.

LITERATURE REVIEWS

1. Rice husk ash

Thailand is an agriculture-based society which produces a large amount of residues from agricultural and forestry sectors. These include rice husk from rice mills of approximately 4.5 million tons per year. Half of rice husk is used as fuel at rice mills or compost. However, the remaining half is mostly piled up to rot or burnt away in open fields, causing various environmental damages.

Rice husk ash is produced from burning rice husks. The amount of silica in rice husk ash depends on combustion conditions. The chemical compositions of rice husk as silica source are shown in Table 1.

Table 1 The chemical compositions of rice husk ash

Composition	Percent (by weight)
SiO ₂	86.9-97.3
K ₂ O	0.58-2.50
Na ₂ O	0.00-1.75
CaO	0.20-1.50
MgO	0.12-0.96
Fe ₂ O ₃	0.00-0.54
P ₂ O ₅	0.20-2.85
SO ₃	0.10-1.13
Others	0.00-0.42

Source: Hanyotee (1999)

Rice husk ash contains over 80% of silica, when it is combusted under an appropriate condition the ash having 70 to 97 percent wt % of amorphous silica is obtained.

Rice husk ash is used as a starting material in mesoporous silica materials synthesis. Mesoporous silicas are majority synthesized from organosilicates such as tetramethyl orthosilicate (TMOS) and tetraethyl orthosilicate (TEOS) as the silica source. These alkoxides are convenient as starting materials but they are expensive.

Thus, the use of raw materials obtained from waste agriculture such as rice husk ash instead of the organosilicates will change the production price of the product and open up new fields of application.

2. Mesoporous materials

Porous solids are used as adsorbents, catalysts and catalyst supports owing to their high surface areas. According to the IUPAC definition, porous materials are divided into three classes: micropore (<2 nm), mesopore (2–50 nm) and macropore (>50 nm) (Sing *et al.*, 1985).. The microporous classes are the zeolites, which give excellent catalytic properties. However, their applications are limited because zeolites have relatively small pore size. This reason becomes limitation in the production of large size products above the dimensions of micro pores. Larger pores are presented in porous glasses and porous gels, which were known as mesoporous materials.

In 1992, Mobil Oil Corporation synthesized the first broad family of mesoporous templated silicates (MTS), the Mobil composite of matter (MCM), based on a liquid-crystal templating mechanism (LCM). Certainly, the discovery of these MCM materials has been a breakthrough in the materials engineering and since then there has been outstanding progress in the development of many new mesoporous solids based on the similar mechanism. The types and physical properties of various mesoporous materials were shown in Table 2.

Table 2 Physical properties of various mesoporous silica materials

Sample code	Structural data		Mean pore size (nm)
	Dimensionality, crystal system and space group	Unit cell dimension (nm)	
MCM-41	2D hexagonal (<i>P6mm</i>)	a = 4.04	3.70
MCM-48	Cubic (<i>Ia3d</i>)	a = 8.08	3.49
FSM-16	2D hexagonal (<i>P6mm</i>)	a = 4.38	2.80
SBA-1	cubic (<i>Pm3n</i>)	a = 7.92	2.00
SBA-2	3D hexagonal (<i>P6₃/mmc</i>)	a = 5.40, c = 8.70	2.22
SBA-3	2D hexagonal (<i>P6mm</i>)	a = 4.75	2.77
SBA-8	2D Rectangular (<i>cmm</i>)	a = 7.57, b = 4.92	1.87
SBA-11	cubic (<i>Pm3m</i>)	a = 10.64	2.50
SBA-12	3D hexagonal (<i>P6₃/mmc</i>)	a = 5.40, c = 8.70	3.10
SBA-14	cubic (<i>Pm3n</i>)	a = 4.47	2.40
SBA-15	2D hexagonal (<i>P6mm</i>)	a = 11.6	7.80
SBA-16	cubic (<i>Pm3m</i>)	a = 17.6	5.40
HMM	2D hexagonal (<i>P6mm</i>)	a = 5.70	3.10
HMM	3D hexagonal (<i>P6₃/mmc</i>)	a = 8.86, c = 5.54	2.70
MSU-1	hexagonal (disordered)	a = 4.73	3.10
MSU-2	hexagonal (disordered)	a = 7.16	3.50
MSU-3	hexagonal (disordered)	a = 7.04	5.80
MSU-4	hexagonal (disordered)	a = 6.01	-
MSU-V	lamellar	a = 3.87	-
MSU-G	lamellar	a = 6.54	3.20
HMS	hexagonal (disordered)	a = 4.55	2.80
KIT-1	hexagonal (disordered)	a = 4.80	3.52
CMK-1	cubic (<i>I4₁32</i>)	a = 8.33	3.00
APO	2D hexagonal (<i>P6mm</i>)	a = 4.27	2.80

Source: Selvam *et al.* (2001)

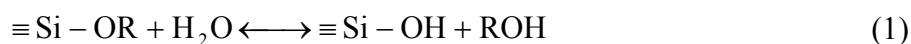
Table 2 shows that these materials have high surface area, with tunable pore sizes in the range 2-50 nm and narrow pore size distributions, which might be controlled the reactant and/or the products.

Regarding these advantages, high demand of these mesoporous molecular sieves for industrial application such as separation, oil refining, petrochemistry, and organic synthesis involving synthesis of large molecule hydrocarbons from small molecules via Fischer-Tropsch synthesis were of interest (Corma *et al.*, 1997; Ohtsuka *et al.*, 2002; 2004). According to the oil crisis and these outstanding characteristics of mesoporous molecular sieves, many researchers have focused on the synthesis of diesel oil from renewable or industrial by products gases. This route of synthesis attracts the researchers in the field of material science and engineering very much.

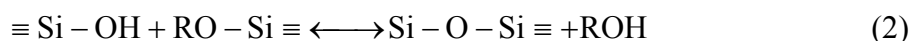
2.1 Chemistry of sol-gel process

The sol-gel preparation of ceramic oxides is a technologically relevant synthetic procedure, which mainly use metal alkoxides as precursors. The preparation occurs via a two-step mechanism, involving the hydrolysis of an alkoxide precursor (formation of the sol) and the subsequent condensation of hydroxyl and/or alkoxy groups (formation of the gel), as shown in Equations 1-3, respectively. The general pathway of a sol-gel process is shown in Figure 1 for silica as a representative ceramic oxide.

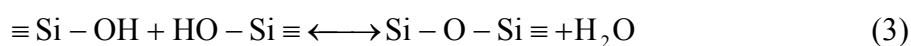
Hydrolysis reaction



Alcohol condensation (silanol- ester condensation)



Water condensation (silanol- silanol condensation)



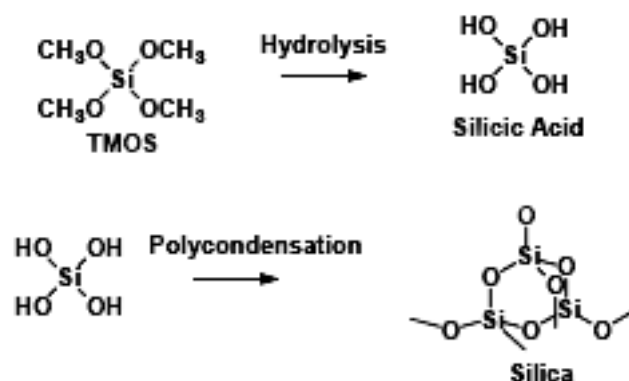


Figure 1 The sol-gel process for the silica network preparation

Source: Chemat Technology (2005)

Mesoporous silica can be synthesized in either the alkaline route or the acid route both using amphiphilic templates. In the acid route, the silica source is silicon alkoxides. The acid catalysis speeds up the hydrolysis versus the condensation rate and promotes mostly condensation at the ends of silica polymers to form linear silicate ions. On the other hand, the alkaline catalysis favors both hydrolysis and condensation. Thus, the alkaline route leads to a highly condensed and compact structure, while the acid route leads to a more fuzzy and soft network. The acid route is popular for studying the morphology, whereas the alkaline route usually provides more stable and ordered materials because silica are highly condensed.

The second important difference is in how the interaction between surfactant and silicates are organized. The isoelectric point of silicate is around $\text{pH} = 2$, below this point the silicate carries a positive charge, whereas in the alkaline route the silicate is negatively charged. So in the alkaline route, surfactant (S^+) and silicates (I^-) organize by the strong S^+I^- electrostatic interaction. In the acid route (with $\text{pH} < 2$), the silica species in solution are positively charged as $\equiv\text{SiOH}^{2+}$ (denoted as I^+). The surfactant-silica interaction becomes $\text{S}^+\text{X}^-\text{I}^+$ as mediated by the counter ion X^- . This micelle-counter ion interaction is in thermodynamic equilibrium. The complex factors one needs to consider are: ion exchange equilibrium of X^- on micellar surface, surface-enhanced concentration of I^+ , and proton-catalyzed silica condensation near micellar surface.

The steps in the synthesis can be roughly separated into two parts: the self-assembly of organic surfactant and the polymerization of inorganic silica. The uncondensed silicate ions serve as the counter ions in the early stage of surfactant self-assembly, this occurs quickly. The silica condensation rate is, however, slower, and the extent of condensation is pH and temperature dependent.

2.2 Chemistry of surfactant in an aqueous solution

The physical chemistry of organized matter relies on the combination of sol-gel chemistry and self-assembly procedures, to control the texture of materials at the nanometer scale. The growth of chemistry-derived inorganic or hybrid networks templated by organized surfactant assemblies (structure directing agents) allows to construct a new kind of materials in the mesoscopic scale.

An amphiphilic molecule or surfactant consists of a hydrophobic hydrocarbon chain and a hydrophilic head group. When mixed with water, “like likes like” is a structure-directing principle in that the surfactant molecules undergo self-assembly into aggregates as micelles that shown in Figure 2 (<http://www.chem.ucalgary.ca>). The structures formed depend on the surfactant concentration and range from the simple spherical micelles to the more complex lyotropic liquid crystal phases.

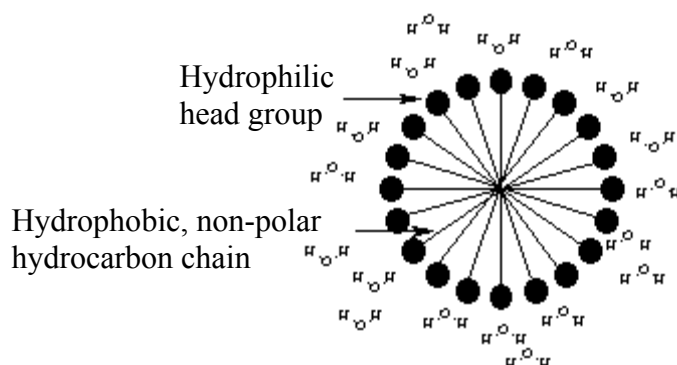


Figure 2 Micellization of surfactant in aqueous solution

Source: University of Calgary (2005)

The choice of the organic template to control the process in the mesoscale is a key issue in the synthesis of textured or porous materials. In the case of mesoporous oxides, the templating relies on supramolecular arrays: micellar systems formed by surfactants or block copolymers (BC) are indeed interesting as supramolecular templates because they are capable to impart larger pores and thicker walls, industrially available, hazard-free and easy to remove.

Block copolymers (BC) are suitable and versatile templates for synthesis of mesoporous materials. During last decade, the ionic surfactants such as cationic alkyltrimethylammonium (C_nTA^+ , $n=8-18$) and anionic alkylsulfonates ($C_nSO_3^{2-}$, $n=12-18$) were used in the synthesis processes of mesoporous oxides. These oxides are synthesized in acidic or basic conditions, yielding materials with controlled pore size between 1.5 to 10 nm. However, ionic surfactants have typical two main limitations: (1) small wall thickness (0.8-1.3 nm), which is a serious limitation regarding stability for catalysis reaction; (2) limited pore size offered by molecular surfactants.

The self-assemble characteristics of BC permit to control the superstructure, to vary the typical length scales and to add specific functions. As a result, the properties of BC can be continuously tuned by adjusting solvent composition, molecular weight or polymer architecture. The typical BC as templates are shown in Figure 3.

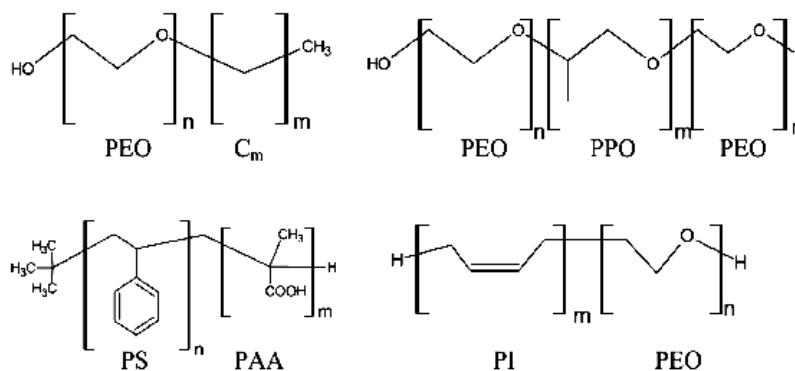


Figure 3 Block copolymer templates used in mesoporous materials

Source: Soler-Illia *et al.* (2003)

Pinnavaia *et al.* (1995) brought the idea of using nonionic surfactants in neutral media. Some advantages of using neutral non-ionic surfactants over the ionic ones were noticed as follows: (1) larger inorganic wall thickness (1.5–4 nm) enhancing the hydrothermal stability of the mesoporous oxides; (2) easier pore diameter tuning by varying both the type and the concentration of the surfactant, (3) easier solvent removal by solvent extraction; H-bonding (instead of electrostatic) interactions between the template and the inorganic framework should be easier to dissociate. Zhao *et al.* (1998) also obtained highly ordered large-pore (4.5–30 nm), thick-wall (3–7 nm) of mesoporous silica by using triblock copolymer as templates [(EO)_n(PO)_m(EO)_n].

2.3 Synthesis of mesoporous materials

Generally, a typical mesoporous silica synthesis, an aqueous solution containing silica, fumed silica, sodium silicate, TEOS, TMOS as the silica source are added to aqueous solution (acid/alkaline) of the micelle-forming surfactant such as block copolymer (tri- or di-) or long chain quaternary ammonium halides under stirred or unstirred conditions at room temperature or higher. Those conditions are effected to the morphologies of materials (rod, ring, fiber, sphere-like). The silica source is hydrolyzed and condensed to multicharged anion or cation form (anion, pH>2 and cation, pH<2) that can be coordinated with the surfactant head groups. The interaction between silicate species and the surfactant is assembled as silica-surfactant phases, and then a mixture solution is formed gel (siloxane network). The gel is transferred into Teflon-lined autoclave and then heated at 70-120°C for 1-3 days. After crystallization, the solid products are filtered from the mixture solutions, washed with distilled water or ethanol and dried in air at room temperature or higher (Selvam *et al.*, 2001). Table 3 shows some structures with their synthesis conditions.

Table 3 Various mesoporous silica based on 2D hexagonal ($P6mm$)

Name	Silica source	Template	Reaction conditions	References
HMP	TEOS	$C_{12}EO_8$	silica/surfactant/water mixture aged for 18 h at RT; surfactant / water=50 wt %	Attard <i>et al.</i>
MCM-41	Sodium silicate	Alkyltrimethylammonium	hydrothermal synthesis at 373 K for 144 h	Beck <i>et al.</i>
FSM-17	sodium kanemite	Cetyltrimethylammonium chloride	silica/surfactant ratio=1:20 (%wt); final pH=11.3; stirred at 353 K for 3 h	Chen <i>et al.</i>
MMS	TEOS	$EO_{106}PO_{70}EO_{106}$	silica/surfactant/butanol/water mixture; hydrothermal synthesis at 373 K for 24 h	Feng <i>et al.</i>
SBA-3	TEOS	Cetyltrimethylammonium bromide + HBr	silica/surfactant/acid/water mixture stirred at RT for ≥ 30 min	Huo <i>et al.</i>
SBA-15	TEOS	$C_{16}EO_{10}$	silica/surfactant/water mixture heated at 373 K for 24 h	Huo <i>et al.</i>
FSM-16	sodium kanemite	Cetyltrimethylammonium chloride	silica/surfactant/water mixture heated at 343 K with stirring; after 3 h, pH adjusted to 8.5, and mixture again heated at 343 K for 3 h	Inagaki <i>et al.</i>
MMS	H_2SiF_6	Cetyltrimethylammonium bromide	silica/surfactant/water mixture (pH=7-8) aged at 343 K for 5 h	Jeong <i>et al.</i>
MSM	$(NH_4)_2SiF_6$	Cetyltrimethylammonium bromide	silica/surfactant/water mixture (pH = 8) stirred at RT for 1 h	Voegtlin <i>et al.</i>
SBA-15	TEOS	$EO_{20}PO_{70}EO_{20}$	silica/surfactant/water mixture heated at 313 K for 24 h	Zhao <i>et al.</i>

Source: Selvam *et al.* (2001)

2.4 Mechanism of mesoporous materials formation

The original inorganic mesoporous material synthesis was carried out in distilled water under base-synthesis condition of which similar to zeolite syntheses. However, the structure directing agents are not a single organic molecules as same as zeolite synthesis but the liquid crystal templating (LCT) molecules. The formation of the inorganic-organic composites is based on electrostatic interactions between the positively charged surfactant (S^+) and the negatively charged silicate species (I^-) in the system.

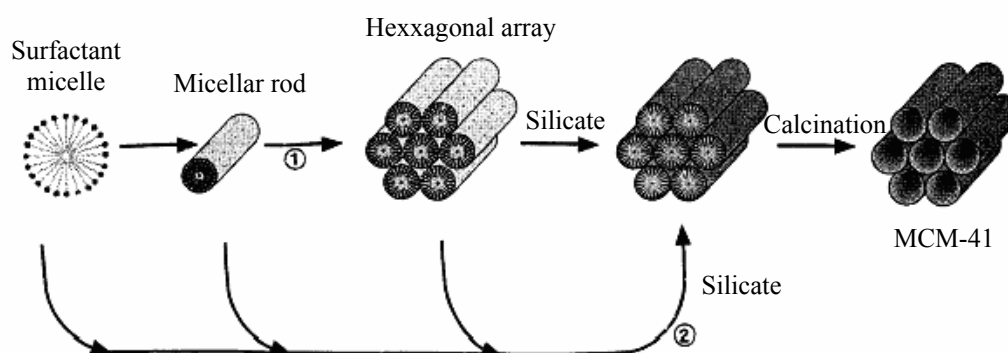


Figure 4 The liquid crystal templating mechanism for the formation of MCM-41:

(1) liquid-crystal-phase-initiated and (2) silicate-anion-initiated

Source: Beck *et al.* (1992)

Beck *et al.* (1992) proposed two possible pathways, in which either the structure directing agents are converted to the liquid crystals before the silica sources are added (pathway 1) or the addition of the silicate results in the ordering of the subsequent silicate-encased surfactant micelles (pathway 2). Several researchers have also investigated the mechanism of mesoporous materials formation (Mou *et al.*, 2000; Flodstrom *et al.*, 2003; Tendeloo *et al.*, 2006; Xia *et al.*, 2004 and Ruthstein *et al.*, 2006).

The physical chemistry of organized matter depends on the complete combination of the sol-gel chemistry and self-assembly procedure, to uniquely control the texture of materials. Choi *et al.* (2003) reported the effect of sol-gel synthesis on SBA-15 with Ploronic P-123 as template, well-ordered mesoporous silica was formed. The scientists have tried to use inexpensive liquid crystal templating for mesoporous silica synthesis. Block copolymer groups are indeed suitable and versatile templates for creation of mesoporous and mesostructured materials. Two main processes are recognized in the formation of these mesophases, which is schematized in Figure 5.

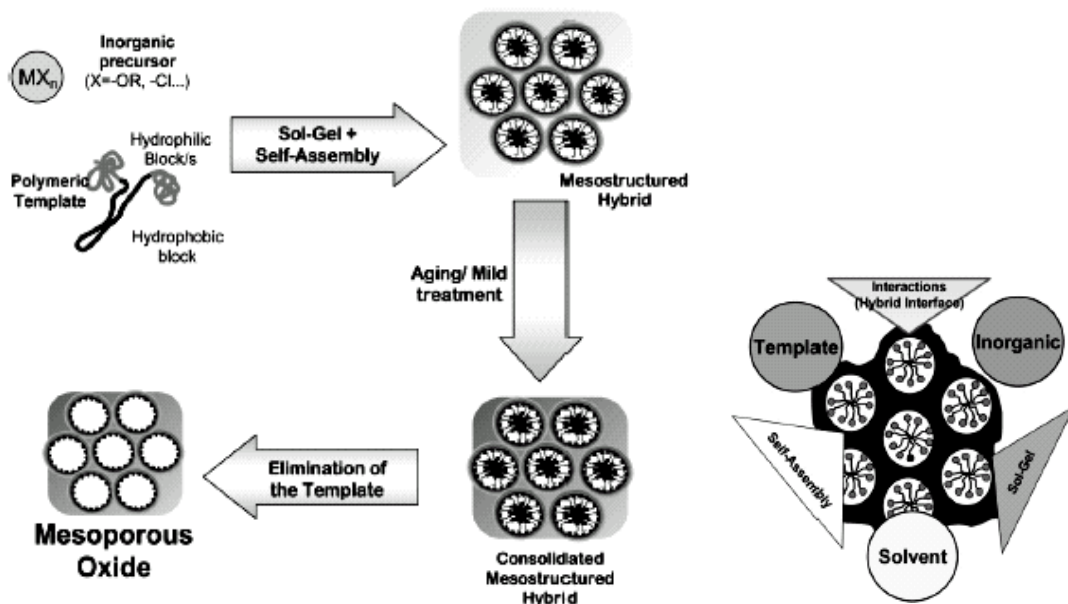


Figure 5 (a) The procedure of a mesoporous oxide network synthesis from the solution and (b) the main relationships of mesostructured hybrid

Source: Soler-Illia *et al.* (2003)

The creation of an organized texture (Figure 5 (a)) is due to the self assemble properties of the template. This process results in a microphase separation, which divides the space in two domains: hydrophilic and hydrophobic, in the case of the simplest BC surfactants.

For the formation of an inorganic network (Figure 5 (b)), the inorganic components are placed in one of the spatially separated parts of these

nanoheterogeneous systems. Condensation reactions will give rise to an extended inorganic network; these reactions can be tuned to take place simultaneously or subsequently as organization proceeds.

2.5 Pore size modification

The generation of different pore sizes (2-50 nm) in mesoporous silica materials can be achieved by varying of the alkyl chain length or PEO/PPO of the surfactant molecules. Group of researchers have investigated the effect of templates on pore size as follows:

Flodstrom *et al.* (2003) studied the influence of different block lengths of Pluronic surfactants, $(EO)_x-(PO)_y-(EO)_x$, under acidic conditions for SBA-15 synthesis. They found that the wall thickness was largely depended on the length of the EO-blocks, while the pore diameter is depended on the length of the PO-blocks.

Jana *et al.* (2004) controlled the pore size of mesoporous silicas by using different organic auxiliary chemicals, such as methyl substituted benzenes (1,3,5-; 1,2,4-; 1,2,3-trimethylbenzenes), isopropyl substituted benzenes (1-; 1,3-di; 1,3,5-triisopropylbenzenes), alkanes (octane, nonane, decane, tridecane, hexadecane, eicosane) and 1-octanol, under hydrothermal conditions. The swelling effect was arranged in order as follows: alkanes < isopropyl substituted benzenes < methyl substituted benzenes. 1-Octanol could not modify the pore size of MCM-41 and SBA-15. The pore diameter of MCM-41 and SBA-15 can be controlled up to 9.1 nm and 43 nm, respectively.

Boissiere *et al.* (2003) synthesized MSU-X mesoporous silica by controlling of various synthesis parameters such as silica concentration, adding of a swelling agent (1,3,5-trimethyl benzene: TMB), condensation catalyst (NaF) and condensation temperature. Pore size distributions were tuned between 2.5 to 5 nm. Example of swelling micelle with 1,3,5-trimethyl benzene was illustrated in Figure 6; with hydrophobicity TMB, the big micelle was obtained.

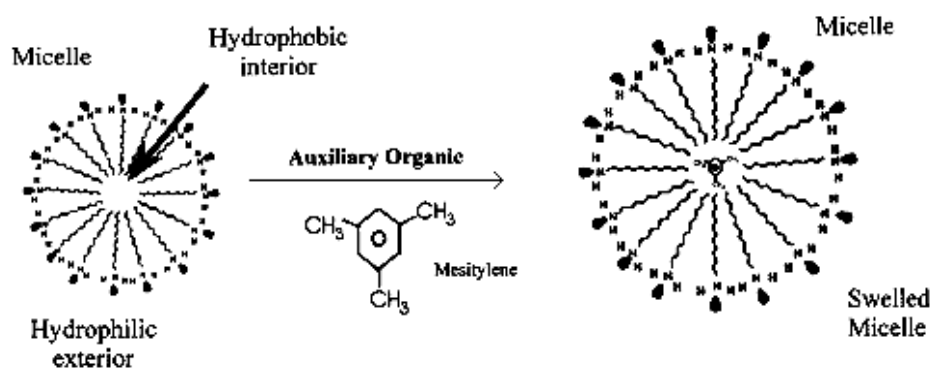


Figure 6 The expansion of surfactant micelle with 1, 3, 5-trimethyl benzene (TMB) as swelling agent

Source: Vartuli *et al.* (1998)

2.6 Factors affecting the modification of mesoporous materials

The modification of ordered mesoporous materials is controlled with a wide range of synthesis variables as follows: 1) surfactant concentrations, 2) temperatures, 3) pH, 4) inorganic precursor types, and 5) additives, which have been affected these syntheses.

2.6.1 Surfactant concentration

Surfactant concentration affects not only micelle formation (CMC) but the regularity and morphology of material oxides.

Beck *et al.* (1992) studied the synthesis, characterization, and proposed mechanism of formation of a new family of silicate/aluminosilicate mesoporous molecular sieves, MCM-41. They found that low surfactant concentrations gave a disordered structure; for all that, the order structure rapidly increased with increasing surfactant concentrations. With increasing the surfactant concentration, the hexagonal structure became progressively more disordered and

wormhole-like structures were obtained. At higher reaching a maximum of surfactant concentrations the order of the mesoporous silica structure again decreased.

2.6.2 Temperatures

The pore sizes of mesoporous materials are greatly affected by temperature changing. Morphologies of material oxides can be controlled by temperatures as shown in the following examples.

Martines *et al.* (2004) synthesized MSU-3 mesoporous silicas from Pluronic P123 with two-step processes. The synthesis temperatures were divided into three ranges: 5-25°C, 35-45°C, and above 45°C. The effect of particles morphology was investigated. Below 25°C, the particles exhibited the spherical shape. From 35 to 45°C, the particle is totally stick-like shape (there is an intermediary stage at 25°C), and above 45°C, the particles loosed their structure and evolved toward a fluffy powder with a growing amorphous part made of very small aggregates of silica. Samples synthesized at 35 and 45°C exhibited a clear set of diffraction peaks that could be assigned to a hexagonal symmetry. From 35 to 45°C, the cell parameter has expanded from 9.2 to 10.8 nm. Form surface area analyzer, surface area varies continuously from 300 to 700 m²/g and porous volume from 0.1 to 1.0 cm³/g, when the synthesis temperature varied from 5 to 65°C.

2.6.3 Amount of acid concentration

The important of amounts of acid concentration on the properties of SBA-15 mesoporous silica synthesized from rice husk ash were studied by Nanta-ngern (2005). He found that at higher 0.00875 mole of Pluronic P123, the amount of HCl concentration had hardly effect on the pore size and surface area of SBA-15 mesoporous silica.

2.6.4 Inorganic precursor types

The several inorganic precursors had been used in the synthesis of mesoporous materials and led to different products. Tetraethyl orthosilicate (TEOS) or tetramethyl orthosilicate (TMOS) are considered as expensive sources of precursor. One example of inexpensive sources is sodium silicate for synthesis of SBA-15 (Corriu *et al.*, 2004). Li *et al.* (2001) used kinemite as the silica source in FSM-16 synthesis. FSM-16 mesoporous silica was reported to have higher thermal and hydrothermal stability than MCM-41.

2.6.5 Swelling agents

Jana *et al.* (2004) synthesized large mesopore SBA-15 and MCM-41 by using four different types of swelling agent as follows: 1) methyl-substituted benzene (1,3,5-, 1,2,4- or 1,2,3-trimethylbenzene); 2) isopropyl-substituted benzene (1-, 1,3-di- or 1,3,5-tri-isopropylbenzene); 3) alkane (octane, nonane, decane, tridecane, hexadecane or eicosane); and 4) 1-octanol under hydrothermal conditions. They found that the swelling agents/silica ratio used for these mesoporous syntheses influenced the pore size of materials in the following order: alkane < isopropyl-substituted benzene < methyl-substituted benzene. The ordered mesopore size decreased when increasing the swelling agents/silica ratio. The BJH pore size of MCM-41 can be controlled up to 9.1 nm and SBA-15 up to 43.0 nm.

Lettow *et al.* (2000) investigated the phase transition between hexagonal SBA-15 and spherical MCF by varying the 1,3,5-trimethylbenzene/Pluronic P123 mass ratios between 0 to 0.5. When the ratio increased, a phase transformed from hexagonal to spherical phase with a transition region of 0.2-0.3 mass ratio.

Blin *et al.* (2000) reported that dodecane can be used as swelling agents to expand the pore size of MCM-41 materials. They studied the dodecane/CTMABr molar ratio from 0 to 2.5 and found that the pore size with BJH

method increase up to 92 %. No XRD peak was observed when these molar ratios increased more than 3.

3. SBA-15 mesoporous silica

SBA-15 periodic mesoporous silica represents a new class of inorganics which discovered by Zhao *et al.* (1998). This SBA-15 is the well-ordered 2-dimensional hexagonal periodic mesoporous silica with high surface area (600-1,000 m²/g), narrow pore size distribution, large pore volume (1-2 cm³/g) and high thermal stability. The pore diameters of SBA-15 can be controlled in the range of 2-30 nm by the modification using various surfactants, some additives and different synthetic conditions (Zhao *et al.*, 2000). At present, SBA-15 mesoporous molecular sieves become more popular because of its characteristics that have larger, thicker pore walls and higher thermal stability when compared with HMS and MCM-41 (Linssen *et al.*, 2003). It is essential in the industrial catalytic applications that the support selectivity and reactivity can be manipulated.

3.1 Synthesis of SBA-15 mesoporous silica

Generally, for a typical SBA-15 mesoporous silica synthesis, an aqueous solution containing silica such as tetraethoxysilane (TEOS), tetramethoxysilane (TMOS), tetrapropoxysilane (TPOS) is used as silica source. An acid media solution of the micelle forming triblock copolymer surfactant is added under stirred conditions at 35-80°C. Then the obtained gel is transferred into autoclave and heated at 70-140°C for 11 to 72 hour. After crystallization, the solid products are filtered, washed with distilled water or ethanol and dry at 140°C for 3 hours and calcined at 500°C for 6 hour. The SBA-15 synthesis processes have also clarified by various groups of researchers.

Zhao *et al.* (1998) studied the triblock copolymer synthesis of mesoporous silica with periodic 5 to 30 nm. They found that SBA-15 mesoporous

silica prepared from PEO₂₀PPO₇₀PEO₂₀ triblock copolymer as template showed high degree of hexagonal mesoscopic organization.

Nanta-ngern (2005) studied the synthesis of SBA-15 mesoporous silica from rice husk ash as silica source and Pluronic P123 as template under strong acidic condition. He found that the synthesized SBA-15 mesoporous silicas had pore volumes of 0.64-2.44 cm³/g, pore diameters of 7.7-13.5 nm, and surface area of higher than 600 m²/g. At higher hydrochloric acid and Pluronic P123 concentrations, the maximum surface areas were increased up to 21.2 and 22.4 % respectively. With Pluronic P123 of lower than 0.02 moles, maximum pore diameters were increased up to 23.4 % and narrow pore size distribution was obtained.

3.2 Characterization of SBA-15 mesoporous silica

The structures of SBA-15 mesoporous silica are characterized by using nitrogen adsorption, Scanning Electron Microscopy (SEM), Transmission Electron Microscopy (TEM) and X-ray Diffraction (XRD) spectroscopy. This section is presented the instrumental analysis techniques of SBA-15 mesoporous silica for the analysis the mesoporous silica types.

3.2.1 Nitrogen adsorption measurement

Nitrogen adsorption measurement was used to analyze pore sizes, specific surface areas and pore size distribution of the solid materials. Figure 7 shows the nitrogen adsorption isotherm of the SBA-15. It indicates as type-IV isotherm of mesoporous material classified by IUPAC and type-A hysteresis loop. The hysteresis loop is associated with the presence of “cylinder shape” pore of rather constant cross section.

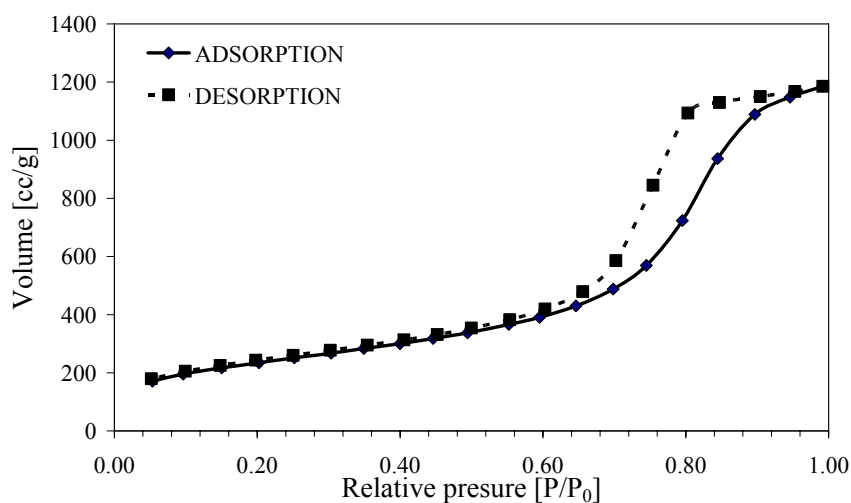


Figure 7 Nitrogen adsorption isotherm of SBA-15 mesoporous silica materials

Source: Nanta-ngern (2005)

3.2.2 Scanning electron microscopy

Scanning electron microscopy (SEM) images for SBA-15 mesoporous silica prepared with Pluronic P123 as template were shown in Figure 8. The SEM observation of SBA-15 mesoporous silica reveals rod-like particles (Zhao *et al.*, 2002).

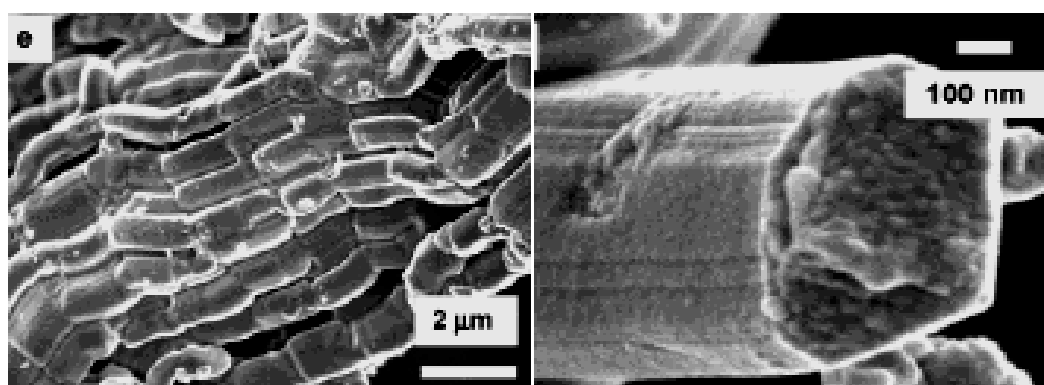


Figure 8 SEM image of SBA-15 mesoporous silica

Source: Zhao *et al.* (2002)

3.2.3 Transmission electron microscopy

Transmission electron microscopy (TEM) is a useful instrument to study the evolution of solid materials synthesis. The TEM image of SBA-15 mesoporous silica was shown in Figure 9. SBA-15 prepared from Pluronic P123 as template also displays the well-ordered hexagonal structure.

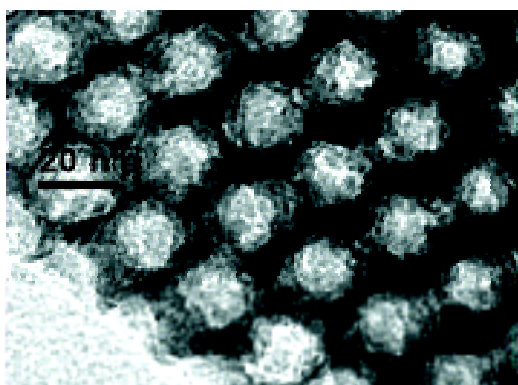


Figure 9 TEM image of calcined hexagonal SBA-15 mesoporous silicas

Source: Zhao *et al.* (2002)

3.2.4 X-ray diffraction spectroscopy

As shown in Figure 10, the XRD pattern of the molecular sieve mesoporous silica shows typically three to five reflections between $2\theta = 2$ and 5° for SBA-15, although samples with more reflections have also been reported.

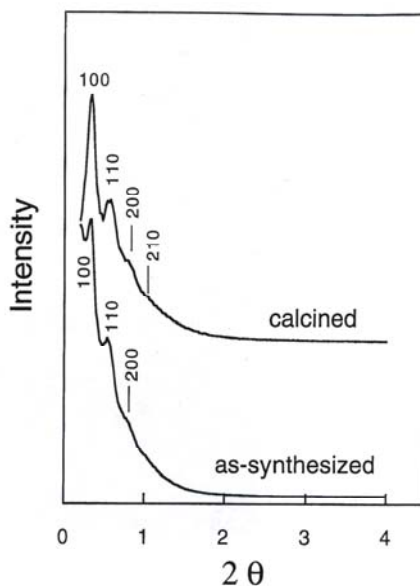


Figure 10 XRD pattern of (A) as synthesized and (B) calcined SBA-15 mesoporous silica

Source: Zhao *et al.* (2002)

The reflections are due to the ordered hexagonal array of parallel silica tubes and can be indexed assuming a hexagonal unit cell as [100], [110], [200], [210] and [300]. Since the materials are not crystalline at the atomic level, no reflections at higher angles are observed (Ciesla *et al.*, 1999).

Due to the characteristics of SBA-15 mesoporous silica that have larger, thicker pore walls and better hydrothermal stability when compared with MCM-41, many researchers have focused on controlling the pore size of SBA-15 mesoporous silica in order to synthesis the valuable chemicals such as long chain hydrocarbons.

3.3 Application of mesoporous silica as catalysts

Mesoporous molecular sieves such as MCM-41, FSM-16 and SBA-15 have large pore volumes, high surface areas, narrow pore size distributions and high thermal stability. Regarding these advantages, high demand of these mesoporous molecular sieves for industrial application such as separation, oil refining,

petrochemistry, and organic synthesis involving synthesis of large molecule hydrocarbons from small molecules via Fischer-Tropsch synthesis were of interest (Corma *et al.*, 1997; Ohtsuka *et al.*, 2002; 2004). According to the oil crisis and these outstanding characteristics of mesoporous molecular sieves, many researchers have focused on the synthesis of diesel oil from renewable or industrial by products gases.

Yin *et al.* (2001) studied the Fischer-Tropsch synthesis by using hexagonal mesoporous silica (HMS) and MCM-41 mesoporous silica as supported Co catalysts. The long chain hydrocarbons (wax) were the main products when mesoporous molecular sieves were used. HMS supported cobalt catalysts showed better catalytic activity and C₅₊ selectivity than those of MCM-41 because HMS have short channel, small pore size and high porosity.

Khodakov *et al.* (2001) studied the pore size effect on Fischer-Tropsch reaction rates and selectivities over a cobalt catalyst at atmospheric pressure by using SBA-15 and MCM-41 mesoporous silicas as catalyst supports. The Fischer-Tropsch reaction rates were found much higher with the pore diameter of over 3 nm than those of narrow pore catalysts. Small pore, MCM-41 led to a small size of the supported cobalt clusters and their lower reducibility in hydrogen atmosphere. It was found that cobalt species located in the narrow pores are less active in Fischer-Tropsch synthesis but very active in methane selectivity.

Ohtsuka *et al.* (2004) used the mesoporous molecular sieves (MCM-41 and SBA-15) with different pore sizes as supports of cobalt catalysts on Fischer-Tropsch synthesis for producing C₁₀-C₂₀ hydrocarbons as the main components of diesel oil. SBA-15 with the pore diameter of 8.3 nm revealed the highest CO conversion and selectivity to C₁₀-C₂₀ hydrocarbons at 523 K, which was higher than the MCM-41 supported cobalt catalyst.

In this research, SBA-15 mesoporous silica synthesized from rice husk ash was modified in order to precisely control the pore size and pore size distribution of SBA-15 by controlling operating conditions in hydrolysis-condensation stage and

hydrothermal treatment stage and, using swelling agent such as 1,3,5-trimethylbenzene (TMB); 2,3,4-trimethylpentane (TMP); tetrahexylammonium bromide (THB) and N,N-dimethyldecylamine (DMD). This SBA-15 mesoporous silica will be applied as the catalyst support for the diesel fuel synthesis via Fischer-Tropsch reaction.

MATERIALS AND METHODS

Materials

1. Sodium hydroxide, NaOH (Merck, Purity of 99 %)
2. Rice husk ash
3. Reagents
 - Distilled water
 - Hydrochloric acid, HCl (J.T. Baker; Purity, 36.5 -38.0 wt %)
 - Pluronic P123, C₅H₁₄O₄ (Aldrich; Product code No. 435-465)
 - Tetrahexyl ammonium bromide, C₂₄H₅₂BrN (Aldrich)
 - N, N-Dimethyl decylamine, C₁₂H₂₇N (Aldrich)
 - 2, 3, 4-Trimethyl pentane, C₈H₁₈ (Aldrich)
 - Mesitylene, C₉H₁₂ (1, 3, 5-Trimethylbenzene) (Fluka; Purity, 98 wt %)
4. Equipment
 - Digital hot plate and stirrer (Schott, SLR)
 - Digital balance (Metler Toledo, AT 400)
 - Furnace (Carbolite, ELF10/6)
 - Electro mantle (Barnstead, EM1000/C)
 - Sieve analysis (Retsch, VIBRO)
 - Ball mill (A-4, MT05)
 - Hot air oven (WTB binder, E.53)
 - pH meter (Schott, CG842)
 - Autoclave
5. Analytical Instrument
 - Surface area and pore size analysis (Quantachrome Corporation, Autosorb-1)
 - Low-angle X-ray Diffractometer (XRD) (Bruker, D8-Advance)
 - Transmission Electron Microscopy (TEM) (TECNAI 20 TWIN)
 - Scanning Electron-Energy Dispersive Spectrometer (SEM-EDS) (JEOL, JSM-530 and JSM-5410)

Methods

The experimental section was divided into four parts as follows: 1) preparation of sodium silicate solution from rice husk ash 2) synthesis and modification of SBA-15 mesoporous silica from sodium silicate solution 3) study of Design of Experiment (DOE) regarding the effect of operating conditions including hydrolysis-condensation temperature, hydrothermal treatment temperature, amount of hydrochloric acid (HCl) and swelling agents on the pore size of synthesized materials and 4) study of the effect of swelling agents. The details of study in each part are:

1. Preparation of sodium silicate solution from rice husk ash

Rice husk ash was prepared using the following methods:

1.1 The rice husk was washed to remove the impurity such as grits, soils and wood scraps.

1.2 One liter of hydrochloric acid (1 M) was added to 50 g of washed rice husk. The mixture was refluxed at 100 °C for 2.5 h.

1.3 The rice husk was then rinsed thoroughly with distilled water and dried overnight in the oven at 120 °C.

1.4 The obtained rice husk was burnt in oxygen atmosphere at 600 °C for 1 h.

1.5 The sodium hydroxide solution was prepared by dissolving 4 g of sodium hydroxide in 29.5 ml of distilled water.

1.6 The rice husk ash of 13.55 g (from (1.4)) was mixed with sodium hydroxide solution and then distilled water was added until the volume of mixture was 100 ml.

1.7 The mixture was then heated up to the temperature of 120 °C and hold at this temperature until the remained volume was 50 ml.

2. Synthesis and modification of SBA-15 mesoporous silica

SBA-15 mesoporous silica materials were synthesized by using triblock copolymer, Pluronic P123 (EO₂₀PO₇₀EO₂₀) as a template and sodium silicate as a silica source under acidic conditions. The molar ratio of 1 SiO₂: 0.00875 Pluronic P123: 200 H₂O: 4HCl was used (Nanta-ngern, 2005). The methods of experiments were as follows:

2.1 The solution of Pluronic P123 was prepared by dissolved 0.00875 mole of Pluronic P123 in 200 mol of distilled water under stirring at room temperature.

2.2 The swelling agents including 1,3,5-trimethylbenzene (TMB), 2,3,4-trimethylpentane (TMP), tetrahexylammonium bromide (THB) and N,N-dimethyldecylamine (DMD) were added in Pluronic P123 solution under vigorous stirring at room temperature. In this stage, the swelling agents/Pluronic P123 were varied in the range of 0-4 g/g.

According to the selection of swelling agents used in this series of experiment, four different chemical structures of swelling agents resulting in the different degrees of polarity were used. The structure of TMB, TMP, THB and DMD were flat coin, branch chain, trigonal pyramid and long chain, respectively. The degrees of polarity are divided into two types as follows: 1) hydrophobic molecules such as TMB and TMP and 2) less hydrophobic molecules such as THB and DMD. From these reasons, the different types of swelling agents should be of significant effect on the pore size of SBA-15. Thus the modification of pore size of SBA-15 mesoporous silica was investigated by using the different types of swelling agents.

2.3 The amounts of hydrochloric acid were added.

2.4 The sodium silicate solution was dropped into the mixture and mixed under vigorous stirring at 30-50°C for 24 h.

2.5 The obtained mixture was placed in the autoclave and heated at 90-120°C for 24 h.

2.6 The solid products were separated from the mixture by filtration and washed with distilled water.

2.7 The products were dried in the oven at 120 °C for 3 h and calcined at 500°C for 6 h. According to the calcination temperature, Zhao *et al.* (1998) who studied the nonionic triblock and star diblock copolymer surfactants for syntheses of highly order mesoporous silicas also used the calcination temperature of 500°C for 6 h to remove the template. Furthermore, Pei *et al.* (2004) who studied the effect of drying of mesoporous structure derived silica with PPO-PEO-PPO template block copolymer, they found that the template was completely eliminated at temperature of 500°C. Therefore, the calcined temperature at 500°C for 6 h was used throughout all the experiment.

After synthesis process, the crystallinity and morphology of SBA-15 mesoporous silicas were characterized by an X-ray diffractometer (XRD), scanning electron micrograph (SEM) and the transmission electron microscopy (TEM), respectively. The surface areas, pore sizes and pore volumes were determined by nitrogen sorption measurements.

3. Factors affecting the synthesis and modification of pore size of SBA-15

The effect of operating conditions including hydrolysis-condensation temperature, hydrothermal treatment temperature, amount of hydrochloric acid and swelling agents on the pore size of synthesise materials were considered. According to various factors affecting the pore size of SBA-15 mesoporous silica, the design of experiments (DOE) approach with factorial 2^k design was considered in order to achieve the optimum condition for synthesis, where the most highly ordered SBA-15 mesoporous silica is produced. The conditions studied for DOE were as follows: hydrolysis-condensation temperature, 30-50°C; hydrothermal treatment, 90-120°C; amounts of HCl and TMB as swelling agent, 3-5 M and 0.5-3 g/g of TMB/Pluronic P123, respectively. The details of experimental design conditions for SBA-15 synthesis are shown in Table 4.

Table 4 Details of experimental design conditions

Run No.	Hydrolysis- condensation temp. (°C)	Hydrothermal treatment temp. (°C)	HCl conc. (M)	TMB/Pluronic P123 (g/g)
1	30	90	3	0.5
2	30	90	3	3
3	30	90	5	0.5
4	30	90	5	3
5	30	120	3	0.5
6	30	120	3	3
7	30	120	5	0.5
8	30	120	5	3
9	50	90	3	0.5
10	50	90	3	3
11	50	90	5	0.5
12	50	90	5	3
13	50	120	3	0.5
14	50	120	3	3
15	50	120	5	0.5
16	50	120	5	3

RESULTS AND DISCUSSION

The results of experiments were divided into five parts as follows: 1) the properties of rice husk ash 2) the DOE study of the effect of operating conditions including hydrolysis-condensation temperature, hydrothermal treatment temperature, amount of hydrochloric acid and swelling agents on the properties of synthesized materials 3) investigation of optimum synthesis condition 4) modification of SBA-15 mesoporous silica using swelling agents and 5) the proposed formation mechanism of SBA-15 obtained from synthesis process using various swelling agents.

1. Rice husk ash

The chemical compositions of rice husk ash (RHA) as the silica source for SBA-15 mesoporous silica synthesis determined by X-ray Fluorescence Spectroscopy (XRF) are mainly composed of SiO_2 (Hanyotee, 1999). The amount of SiO_2 in RHA was 99.6 wt.%. Furthermore, it was found that RHA is highly amorphous solid as can be seen from the XRD pattern as shown in Figure 11. Since silica in RHA was totally amorphous, therefore it can be easily dissolved by sodium hydroxide and formed sodium silicate solution as mentioned by Chareonpanich *et al.* (2004).

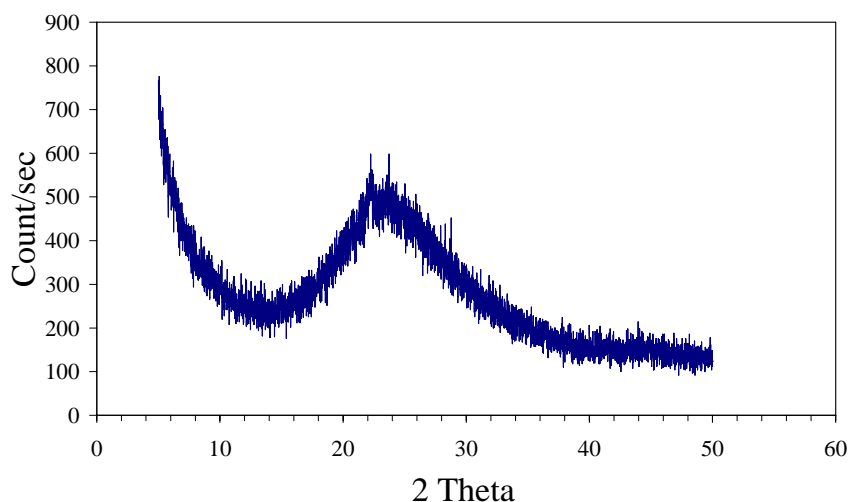


Figure 11 XRD pattern of rice husk ash

Moreover, the nitrogen sorption data shows medium BET surface area, low total pore volume and small average pore diameter as $200 \text{ m}^2/\text{g}$, $0.37 \text{ cm}^3/\text{g}$ and 4 nm , respectively. Figure 12 exhibits relatively wide pore size distribution of RHA which can be classified by IUPAC as the mesoporous material.

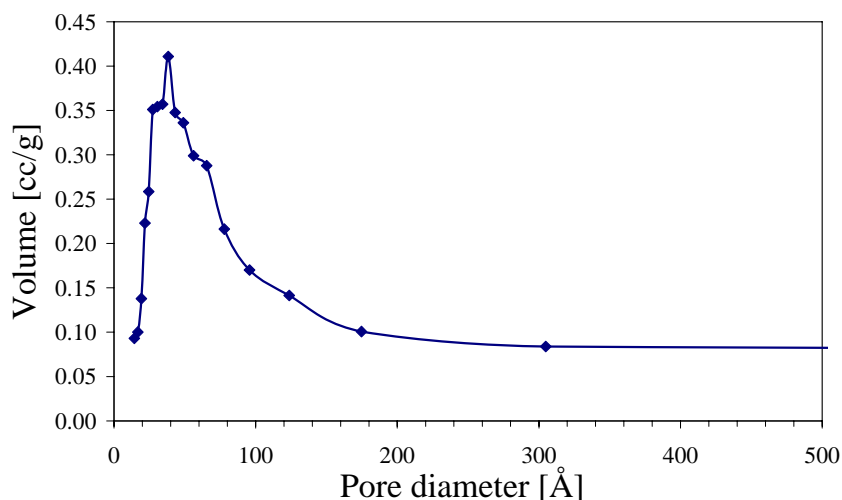


Figure 12 Pore size distribution of rice husk ash

2. Design of experiments (DOE)

The effect of operating conditions including hydrolysis-condensation temperature, hydrothermal treatment temperature, amount of HCl and swelling agents on the properties of synthesized materials were considered. According to various factors affecting the properties of SBA-15 mesoporous silica, the DOE was applied for studying these factors in order to achieve the optimum condition for synthesis. The detail conditions for DOE study were as follows: hydrolysis-condensation temperature, $30\text{-}50^\circ\text{C}$; hydrothermal treatment temperature, $90\text{-}120^\circ\text{C}$; amounts of HCl and TMB as swelling agent, $3\text{-}5 \text{ M}$ and $0.5\text{-}3 \text{ g/g}$ of TMB/Pluronic P123, respectively.

Factorial designs of four factors were consisted of hydrolysis-condensation temperature (A), hydrothermal treatment temperature (B), amounts of HCl (C) and amounts of TMB (D). Higher and lower values of each factor were used in 2^k experimental design method. Hence, the experiments were designed as 16 batches for

investigating the interaction of these factors. According to the principle of DOE, the increased distance between the low and high factor levels results in a reasonable estimate of the essential factor effect.

By nitrogen sorption analysis, the synthesized SBA-15s prepared under the synthesis conditions have pore size of 11-31 nm, surface area of 406-886 m²/g and pore volumes of 0.41-3.15 cm³/g. From the experimental results, the influence of the factors (hydrolysis-condensation temperature (A), hydrothermal treatment temperature (B), amounts of HCl (C) and amounts of TMB (D)) and of their interactions on the response can be obtained from the results of 2⁴ factorial design as presented in Figures 13 and 14.

The surface area and pore size data are plotted between % normal probability and factor effect as shown in Figures 13 and 14 (the detail of DOE calculation is shown in appendix A). All of the effects that lie along or close to the correlation line are negligible, whereas the significant effects are located far away from the correlation line along the x-axis.

2.1 Pore size response

Pore size data from Figure 13 shows that the significant effects can be arranged in the order of importance as follows: $A * B * C * D > B > B * C > B * C * D > A * B * C \gg$ others remaining effects.

As the DOE results, effect of A, C, D and the other interactions can be neglected.

From this result, it indicates that all the factors including hydrolysis-condensation temperature (A), hydrothermal treatment temperature (B), amounts of HCl (C) and amounts of TMB (D) have significant effect on the pore size.

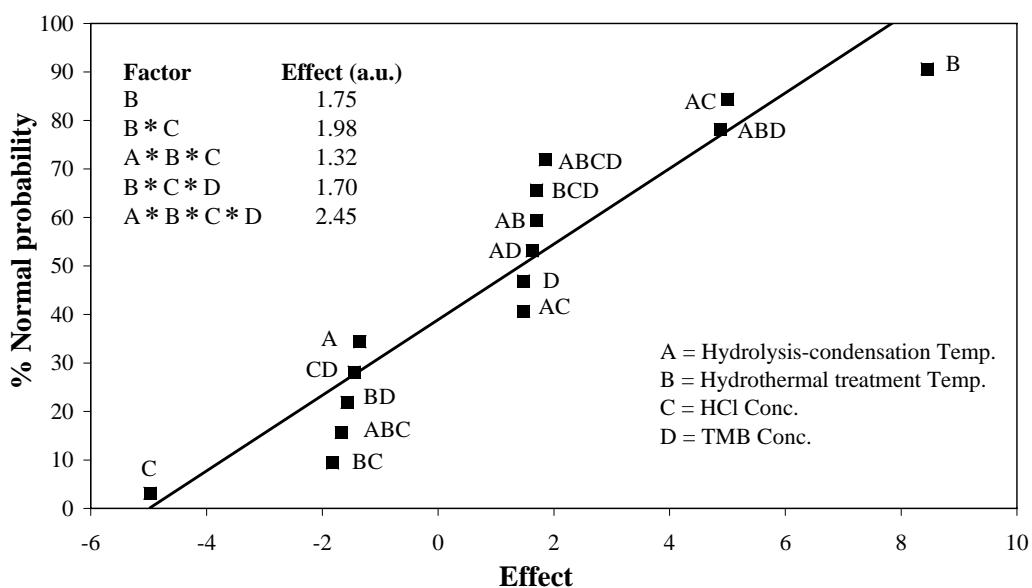


Figure 13 Normal probability plot of the effects for the 2^4 factorial on the pore size

2.2 Surface area response

After evaluating the result of pore size response, the parameter was then compared to the surface area response, we found that the important effects obtained from this analysis are as follows: A and B > A * B * C * D > A * B * C >> others remaining effects.

According to the observed pore size response and surface area response, the factors effect on the textural properties of SBA-15 are hydrolysis-condensation temperature (A), hydrothermal treatment temperature (B), amounts of HCl (C) and amounts of TMB (D).

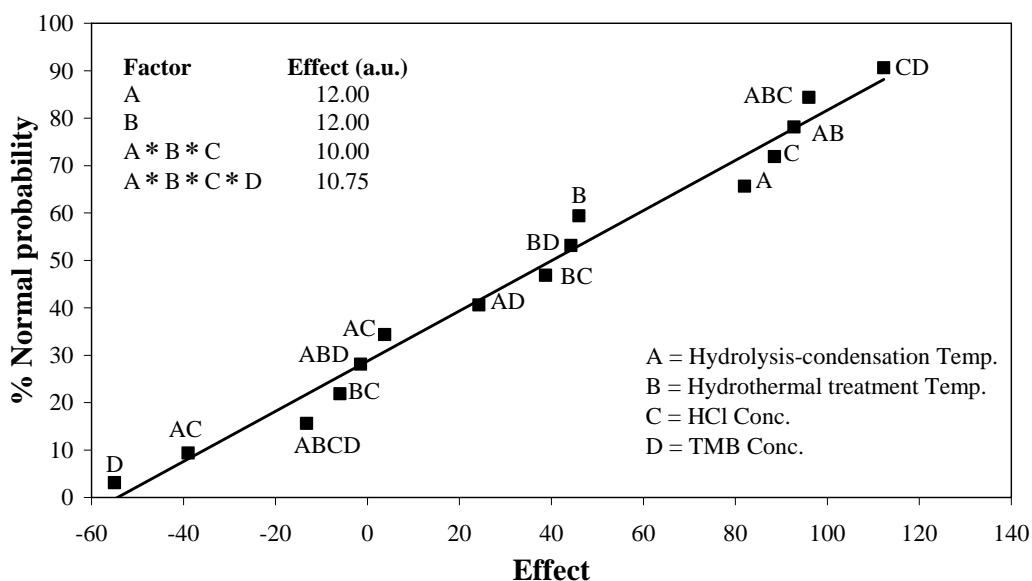


Figure 14 Normal probability plot of the effects for the 2^4 factorial on the surface area

According to Nanta-ngern (2005) who studied the effect of HCl concentrations on the pore size of SBA-15 at 0.00875 mole of Pluronic P123, he found that the amount of HCl had the great effect on the surface area but few effects on the pore size of SBA-15, while the amount of TMB as the swelling agent had the great effect on the pore size and surface area of SBA-15 (Zhao *et al.*, 1998; Jana *et al.*, 2004; Luechinger *et al.*, 2005; Marczewska *et al.*, 2005 and Nanta-ngern, 2005).

From DOE study, the result displays that the amount of HCl and swelling agent have effect on the properties of SBA-15 mesoporous silica. This result is in good agreement with the other researchs. Thus, amount of HCl was fixed at 4 M throughout this study and the amount of swelling agents was varied at 0-4 g/g of TMB/Pluronic P123 in the modification of pore size section.

Therefore, the hydrolysis-condensation temperature and the hydrothermal treatment temperature are selected for the further investigation of the optimum synthesis condition.

3. The optimum synthesis condition

In this section, effects of hydrolysis-condensation temperatures and the hydrothermal treatment temperatures on the properties of SBA-15 mesoporous silicas were investigated. The molar ratio of 1 SiO₂ : 0.00875 Pluronic P123 : 200 H₂O : 4 HCl was used throughout this series of experiment.

The hydrolysis-condensation temperatures were varied as follows: 30, 35, 40 and 50°C while the hydrothermal treatment temperatures were varied at 90, 100, 110 and 120°C. Both reaction periods were fixed at 24 h and 4 M HCl was used to adjust pH of the mixture.

3.1 Nitrogen adsorption

Nitrogen adsorption measurement was used to analyze pore sizes, pore size distributions and specific surface areas of the solid materials. Pore size distributions of SBA-15 mesoporous silica obtained from various hydrolysis-condensation temperatures at the hydrothermal treatment temperatures of 90, 100, 110 and 120°C are shown in Figures 15, 16, 17 and 18, respectively.

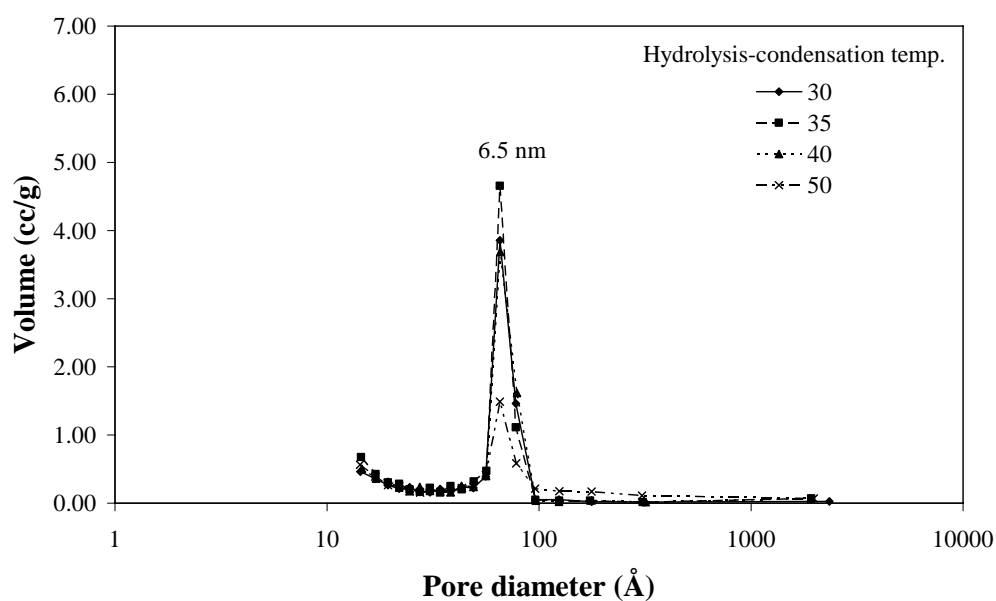


Figure 15 Pore size distribution of SBA-15 mesoporous silica obtained from various hydrolysis-condensation temperatures at the hydrothermal treatment temperature of 90°C

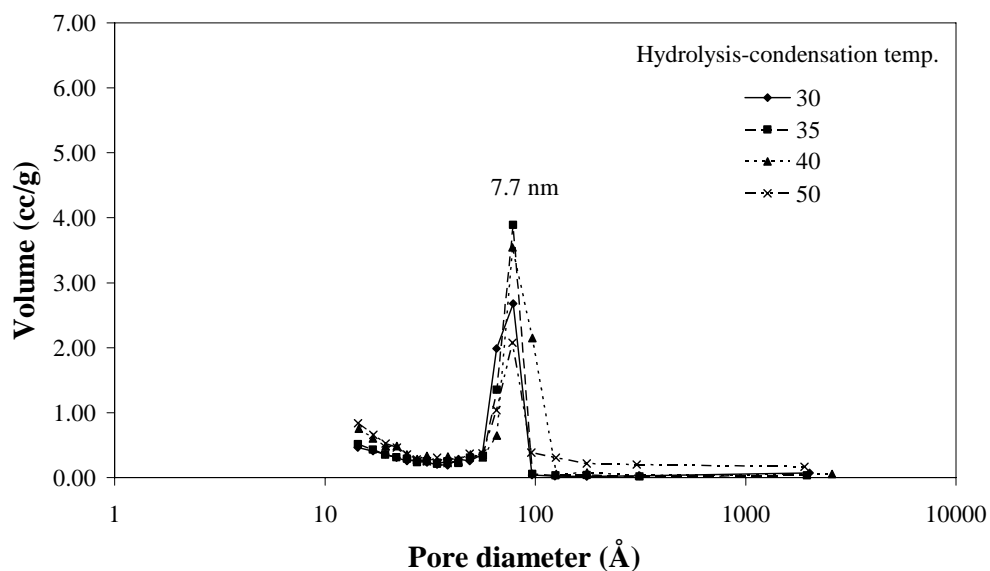


Figure 16 Pore size distribution of SBA-15 mesoporous silica obtained from various hydrolysis-condensation temperatures at the hydrothermal treatment temperature of 100°C

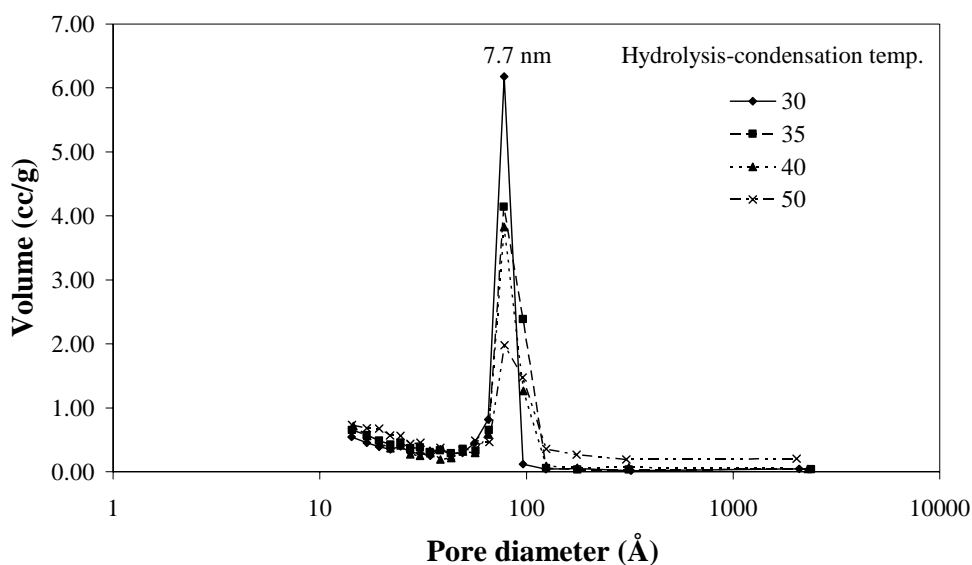


Figure 17 Pore size distribution of SBA-15 mesoporous silica obtained from various hydrolysis-condensation temperatures at the hydrothermal treatment temperature of 110°C

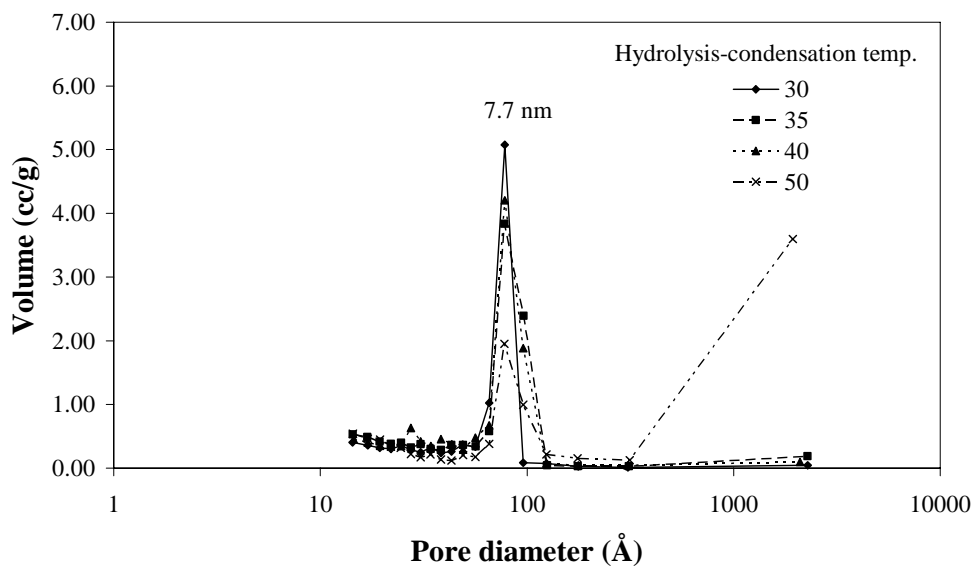


Figure 18 Pore size distribution of SBA-15 mesoporous silica obtained from various hydrolysis-condensation temperatures at the hydrothermal treatment temperature of 120°C

All the products obtained using the hydrolysis-condensation temperature of 50°C exhibit broad pore size distribution. The result indicates that the hydrolysis-condensation temperature at 50°C may cause the disordered pore structure. The similar result was also found by Martines *et al.* (2004). This result can be explained as follows:

The properties of Pluronic P123 can be divided by its structure as two parts: polyethylene oxide (PEO) and polypropylene oxide (PPO) parts, PEO is a strong hydrophilic (water loving) moiety and PPO is a strong hydrophobic (water fearing) moiety. The interactions of PEO and silica polymer are based on H-bonding in the system. At low temperature, PEO segments are strong hydrophilic causing strong H-bonding between PEO segments and the silanol groups (Si-OH), lead to ordered structure. At high temperature, PEO segments become more hydrophobic causing weak H-bonding between PEO segments and the silanol groups, lead to disordered structure of SBA-15 mesoporous silica (Melosh *et al.*, 1999). The influence of temperature has effect on the interaction forces. Increasing of temperature makes internal energy of molecules increase, whereas the interaction forces decrease. Therefore, the interaction force of H-bonding is decreased.

SBA-15 mesoporous silica obtained from the hydrolysis-condensation temperature at 30, 35 and 40°C and the hydrothermal treatment temperature at 110°C have narrow pore size distribution. Figures 19, 20, 21 and 22 show the effect of the hydrolysis-condensation temperature and the hydrothermal treatment temperature on the surface area, pore volume, micropore volume and pore size of SBA-15 mesoporous silica, respectively.

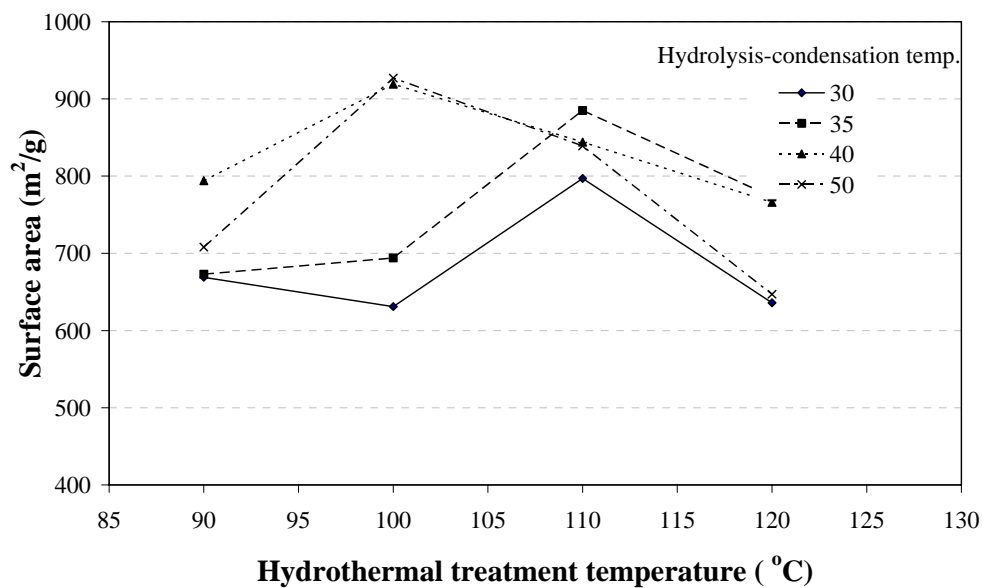


Figure 19 Effect of hydrothermal treatment temperatures and hydrolysis-condensation temperatures on the surface area of SBA-15 mesoporous silica

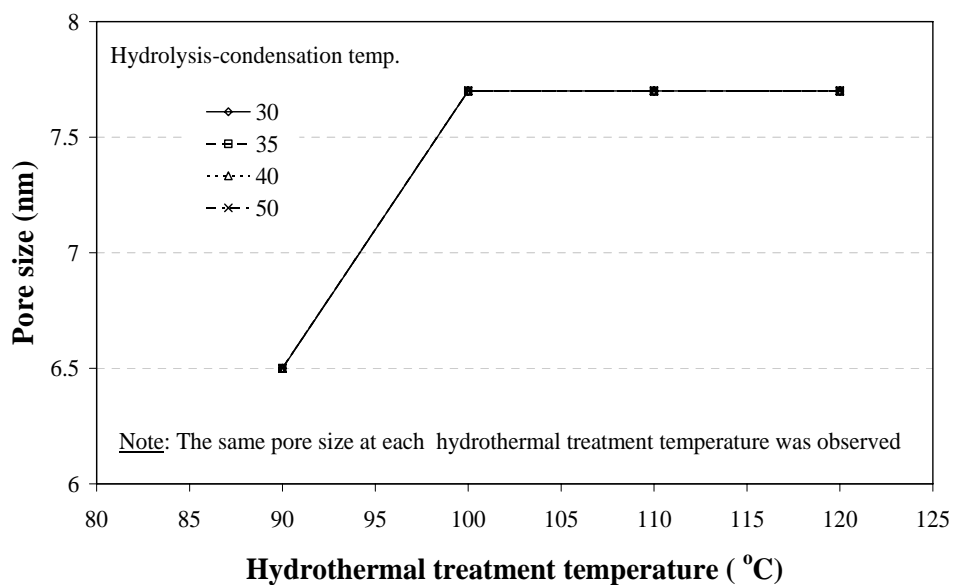


Figure 20 Effect of hydrothermal treatment temperatures and hydrolysis-condensation temperatures on the pore volume of SBA-15 mesoporous silica

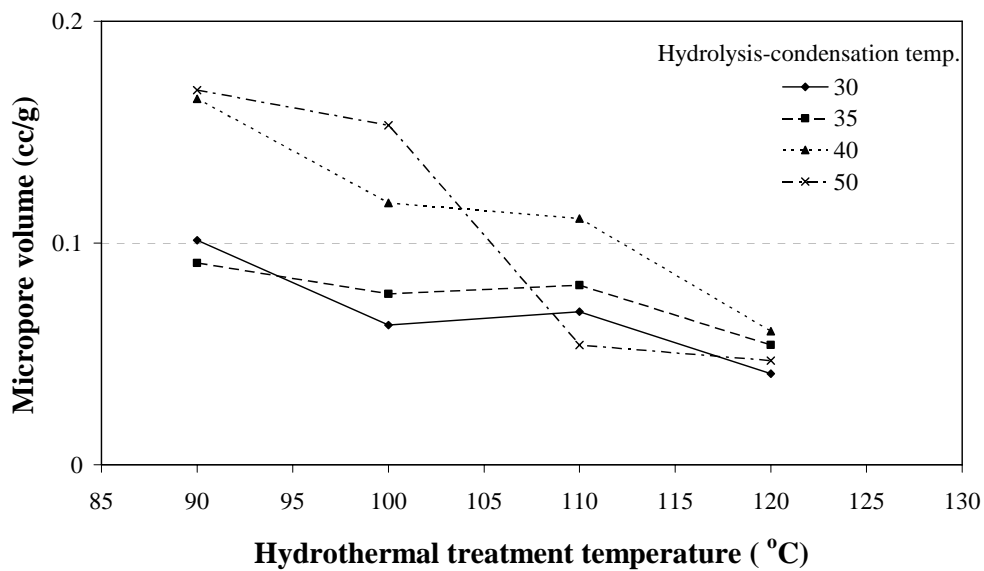


Figure 21 Effect of hydrothermal treatment temperatures and hydrolysis-condensation temperatures on the micropore volume of SBA-15 mesoporous silica

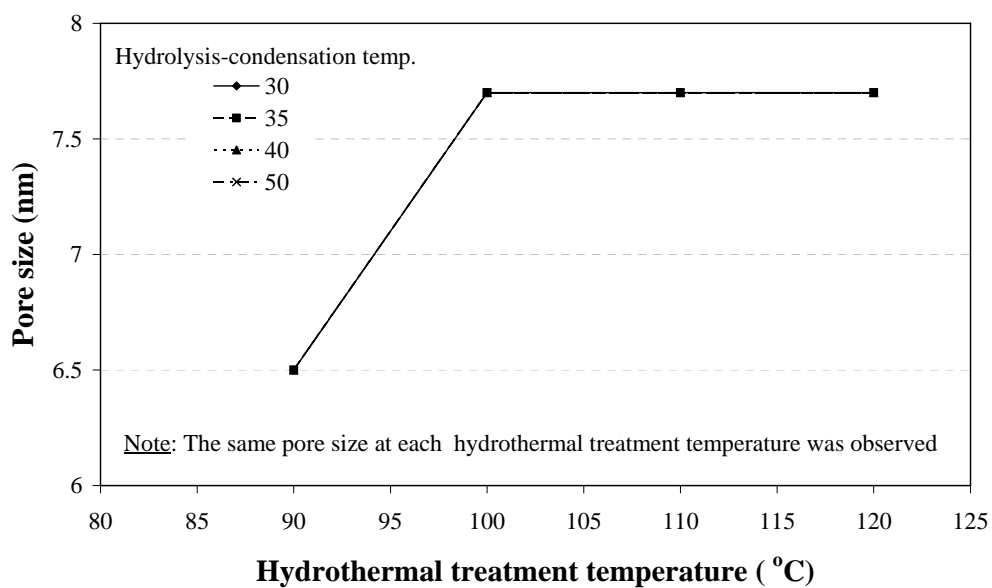


Figure 22 Effect of hydrothermal treatment temperatures and hydrolysis-condensation temperatures on the pore size of SBA-15 mesoporous silica

Both the hydrolysis-condensation temperature and hydrothermal treatment temperature have great effect on the surface area, pore volume and micropore volume of SBA-15 while the pore size is rather constant at 7.7 nm.

As shown in Figures 19 and 20, at lower hydrolysis-condensation temperatures (30 and 35°C), the surface area and pore volume increase with the increase of the hydrothermal treatment temperature up to 110°C, after 120°C a strong decrease of surface area and pore volume are observed. Marczewska *et al.* (2005) also found the similar result. It can be explained that the silica network as a siloxane group ($\equiv\text{Si-O-Si}\equiv$) are linked together, however incomplete linkages are found at the lower hydrolysis-condensation temperature. As increasing the hydrothermal treatment temperature (within 110°C), silica network may occur more than that of lower temperature. The hydrothermal treatment temperature of 120°C, siloxane group tends to be hydrolyzed to form silanol (Si-OH), and causes the decrease of surface area and pore volume. The similar result was also found by Lettow *et al.* (2000) and Marczewska *et al.* (2005).

At higher hydrolysis-condensation temperature (40 and 50°C), the surface area and pore volume increase rapidly with the increase of hydrothermal treatment temperature until 110°C, after that the surface area and pore volume tend to decrease. The result indicates that at high hydrolysis-condensation temperature and high hydrothermal treatment temperature of 100°C, the complete linkages between silica network are formed. Also at higher temperature ($>100^\circ\text{C}$) of the hydrothermal treatment, the silica network can be hydrolyzed to form silanol (Si-OH), and causes the decrease of surface area and pore volume.

As shown in Figure 21, micropore volumes also decrease with increasing the hydrothermal treatment temperatures. This leads to the improvement of the ordered-mesopore of SBA-15 products. Micropore volumes decrease with increasing the hydrothermal treatment temperatures because PEO segments become more hydrophobic and as the result PEO segments are then excluded from silica framework.

Since the results from nitrogen adsorption analysis (Figures 17, 19, 20, 21 and 22) of SBA-15 mesoporous silica at the hydrolysis-condensation temperatures of 30, 35 and 40°C and the hydrothermal treatment temperature of 110°C show narrow pore size distribution, high surface area and pore volume, further analysis including XRD, TEM and SEM analysis were then performed.

3.2 Small-angle X-ray scattering

Small-angle X-ray scattering (SAXS) was used to define mesoporous phase of materials. The SAXS patterns of SBA-15 mesoporous silicas obtained from various hydrolysis-condensation temperatures (30, 35 and 40°C) at the hydrothermal treatment at 110°C are shown in Figure 23.

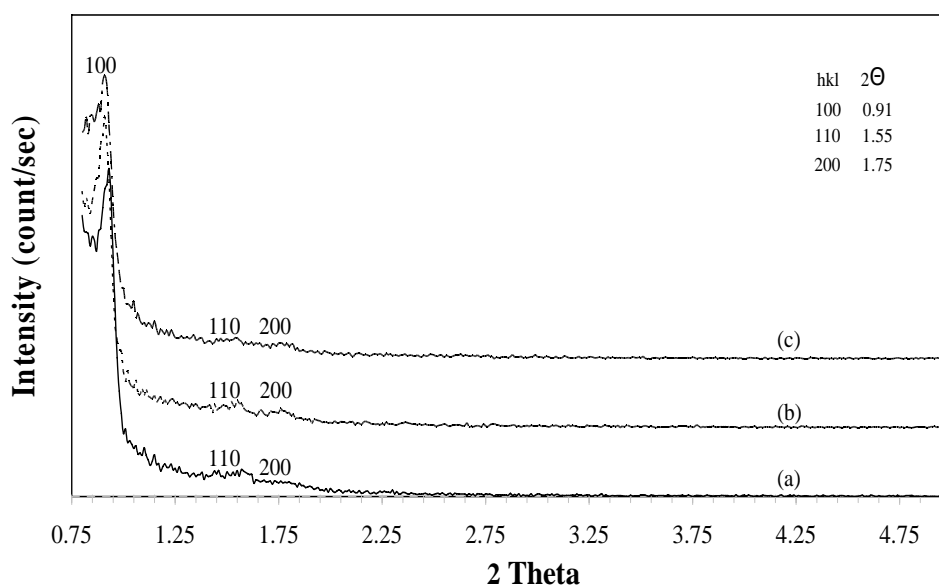


Figure 23 Small-angle X-ray scattering patterns of SBA-15 mesoporous silica obtained from the hydrolysis-condensation temperature at (a) 30°C (b) 35°C and (C) 40°C at the hydrothermal treatment temperature of 110°C

The XRD patterns of SBA-15 obtained from the hydrolysis-condensation temperatures at 35 and 40°C display the [100], [110] and [200] diffraction peaks at 2 Theta values between 0.91-1.75° that can be assigned to the well-ordered hexagonal

structure of mesoporous silica, while that of 30°C shows only two weak diffraction peaks at [100] and [110], indicates the formation of poorly ordered mesoporous silica. From this result, it can be concluded that the increase of the hydrolysis-condensation temperature has great effect on the ordered structure of SBA-15 mesoporous silica and therefore the temperature of 35°C is suitable for SBA-15 synthesis.

3.3 Transmission Electron Microscopy

Transmission electron microscopy (TEM) is a useful instrument to study the evolution of solid materials synthesis. The TEM images of SBA-15 mesoporous silica prepared from the hydrolysis-condensation temperatures of 30, 35 and 40°C and the hydrothermal treatment temperature of 110°C are shown in Figures 24, 25 and 26, respectively.

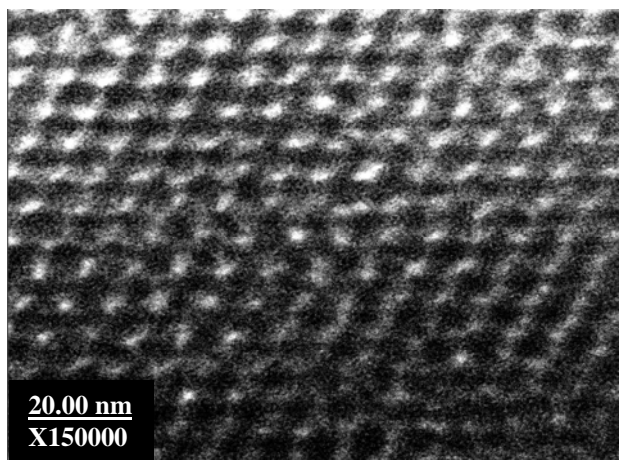
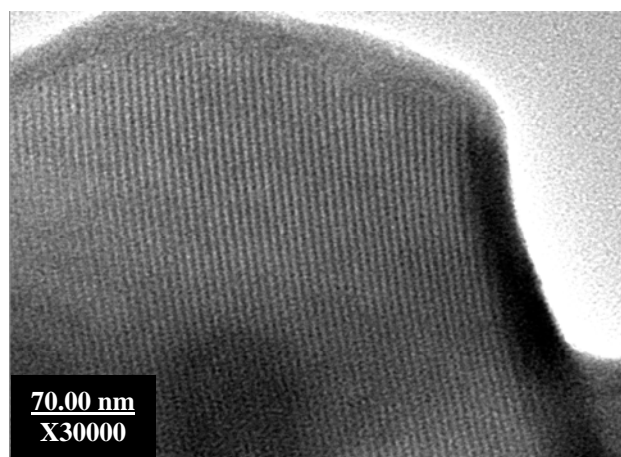
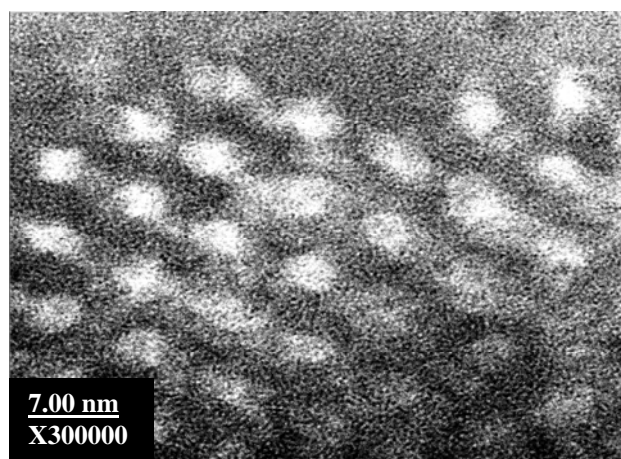


Figure 24 TEM image of SBA-15 mesoporous silica obtained from the hydrolysis-condensation temperature of 30°C and the hydrothermal treatment temperature of 110°C



(a)



(b)

Figure 25 TEM image of (a) perpendicular c-axis and (b) perpendicular a-axis of hexagonal lattice SBA-15 mesoporous silica obtained from the hydrolysis-condensation temperature of 35°C and the hydrothermal treatment temperature of 110°C

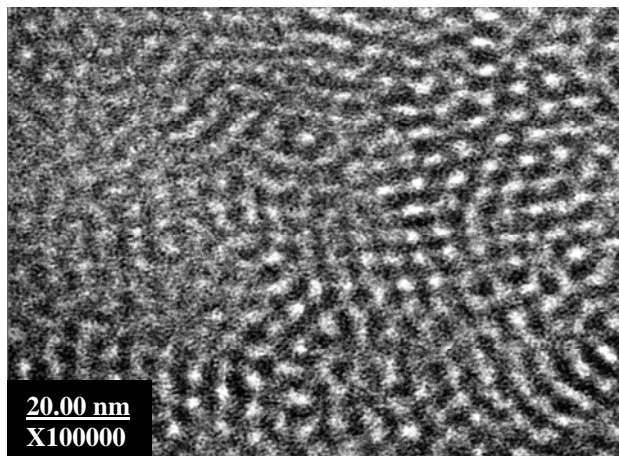


Figure 26 TEM image of SBA-15 mesoporous silica obtained from the hydrolysis-condensation temperature of 40°C and the hydrothermal treatment temperature of 110°C

The TEM images in Figures 24-26 clearly display the 2-dimensional hexagonal structure of SBA-15 mesoporous silica. The behavior of the phase formation changes when the temperature increases. Flodstrom *et al.* (2003) also found the similar result. The well-ordered hexagonal structure of SBA-15 mesoporous silica obtained at hydrolysis-condensation temperature of 35°C is more than that of 30°C. This is because the polymerization reaction may be continued, leads to a more polymerized silica network and this is essential for the formation of highly ordered hexagonal structure of SBA-15 mesoporous silica. The increasing temperature to 40°C can be resulted as the phase transformation due to the dissolution of the silica network (Flodstrom *et al.*, 2003; Marczewska *et al.*, 2005).

3.4 Scanning Electron Microscopy

The SEM images of SBA-15 mesoporous silica obtained from the hydrolysis-condensation at 30, 35 and 40°C are shown in Figures 27, 28 and 29, respectively.

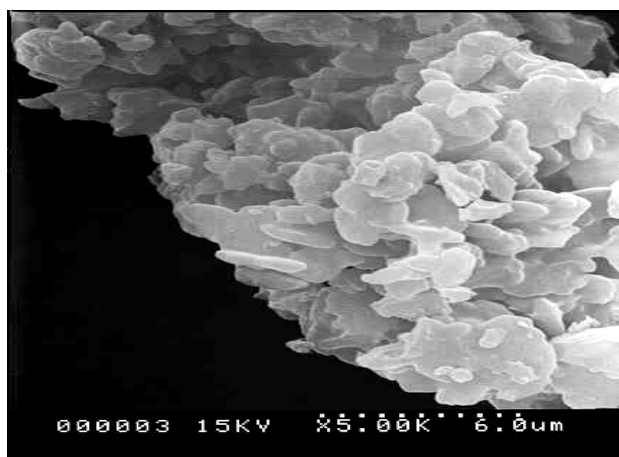


Figure 27 SEM image of SBA-15 mesoporous silica obtained from the hydrolysis-condensation temperature of 30°C and the hydrothermal treatment temperature of 110°C

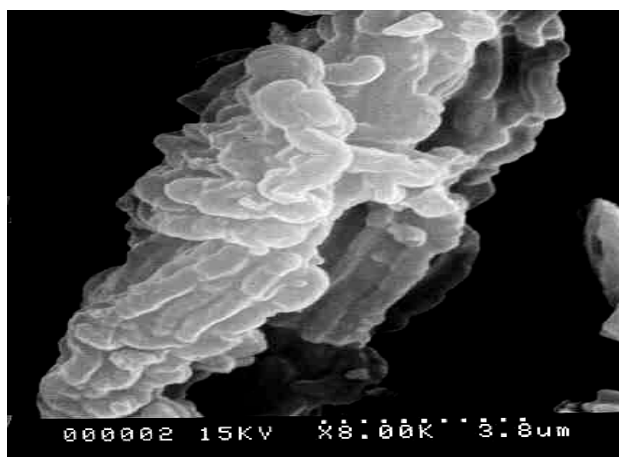


Figure 28 SEM image of SBA-15 mesoporous silica obtained from the hydrolysis-condensation temperature of 35°C and the hydrothermal treatment temperature of 110°C

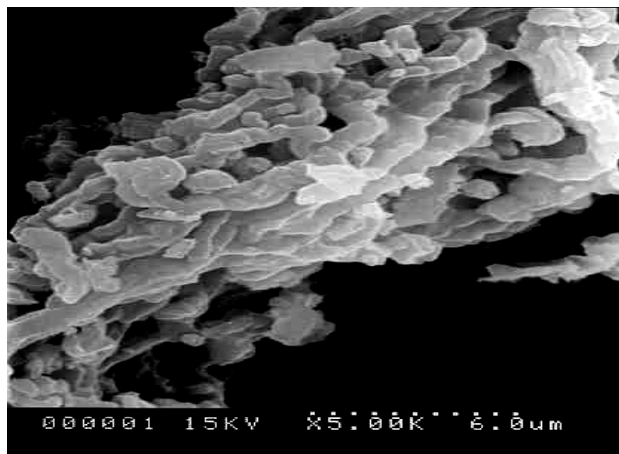


Figure 29 SEM image of SBA-15 mesoporous silica obtained from the hydrolysis-condensation temperature of 40°C and the hydrothermal treatment temperature of 110°C

From Figures 27-29, it can be observed that the morphology of SBA-15 mesoporous silica is hardly depended on the hydrolysis-condensation temperature in the range of our study. However, the SBA-15 obtained from hydrolysis-condensation at 30°C exhibits irregular shape, while the SBA-15 obtained at 35 and 40°C exhibit the oval-like shape. Furthermore, the results observed from low angle XRD and SEM also confirm the phase transformation during the temperature increased. The hexagonal phase is transformed into cubic phase. Our result is in good agreement with those of Flodstrom *et al.* (2003), Kleitz *et al.* (2003), Xia *et al.* (2004) and Marczewska *et al.* (2005).

The data obtained from N₂ adsorption technique, XRD, TEM and SEM reveals the well-defined SBA-15 mesoporous silica obtained at the hydrolysis-condensation temperature at 35°C and the hydrothermal treatment temperature at 110°C. At this condition, SBA-15 mesoporous silica has high specific surface (885 m²/g) area, total pore volume (0.31 cm³/g) (as shown in Figures 19 and 20) and well-ordered hexagonal structure (as shown in Figures 23 and 25). Therefore, this hydrolysis-condensation temperature at 35°C and the hydrothermal treatment

temperature at 110°C is selected for the further investigation of the pore size modification of SBA-15 mesoporous silica throughout this study.

4. Modification of pore size of SBA-15 mesoporous silica

In this series of experiment, the pore size of SBA-15 mesoporous silica was modified by using swelling agents including TMB, TMP, THB and DMD. The swelling agents were added at the ratio of 0-4 (g/g) of swelling agents/Pluronic P123 under acidic condition. The molar ratio of SiO₂ : Pluronic P123 : H₂O : HCl was 1 : 0.00875 : 200 : 4. Since the hydrolysis-condensation temperature and the hydrothermal treatment temperature are suitable for TMB as the swelling agent, it should be noted here that types of swelling agent might not affect these temperatures. Therefore, the hydrolysis-condensation temperature and the hydrothermal treatment temperature were fixed at 35°C and 110°C, respectively. Both of reaction periods were 24 h. The physical properties of swelling agents are shown in Table 5.

Table 5 Physical properties of various types of swelling agents

Name	Phase (At room temp.)	Boiling point (°C)	Melting point (°C)
1,3,5-Trimethylbenzene (TMB)	Liquid	163-166	-45
2,3,4-Trimethylpentane (TMP)	Solid	113-114	-110
Tetrahexylammonium bromide (THB)	Solid	Decomposed	97
N, N-dimethyldecylamine (DMD)	Liquid	234	-

Source: Sigma-Aldrich (2005)

4.1 1,3,5-Trimethylbenzene (TMB) as swelling agent

As shown in Figure 30, pore diameter of SBA-15 mesoporous silica increases with increasing the amount of TMB. Pore diameter of TMB increases about 3 times when the molar ratio of TMB/Pluronic P123 was increased from 0-4 g/g. Pore diameters can be maximally expanded with TMB swelling agent to approximately 31 nm when 3 g/g of TMB was used. At higher than 3 g/g of TMB/Pluronic P123, excess amounts of TMB may form droplets in mixture. The TMB droplets are then encapsulated by silica network, and as a result, SBA-15 surface area is increased. At maximum pore diameter, surface areas again decrease due to a structural collapses during the calcination step. Luechinger *et al.* (2005) studied the effect of the hydrophobicity of aromatic swelling agents on pore size and shape of mesoporous silica. They also found that a small amount of TMB as swelling agent approximately gave mesoporous materials with increased pore diameters and surface areas.

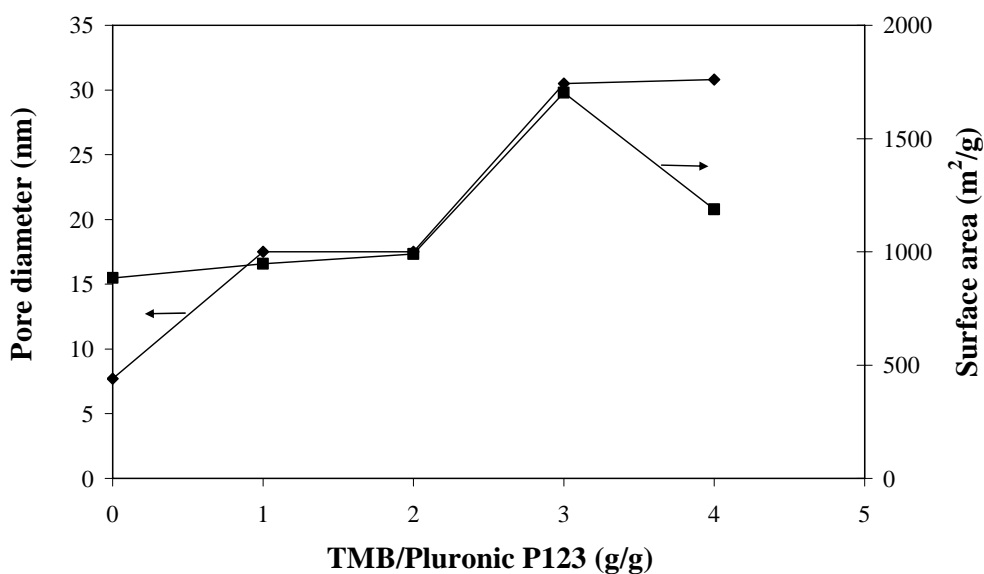


Figure 30 Effects of 1,3,5-trimethylbenzene (TMB) on pore diameter and surface area of SBA-15 mesoporous silica

4.2 2,3,4-Trimethylpentane (TMP) as swelling agent

In the case of 2,3,4-trimethylpentane as shown in Figure 31, we found that the pore diameter of SBA-15 increases with increasing amount of TMP. Pore diameter is increased about 29 times of without swelling agent when increasing TMP/Pluronic P123 from 0 to 4 g/g. At lower than 2 g/g of TMP/Pluronic P123, pore diameter slowly increases from 7.7 to 12 nm, then significantly increases at TMP/Pluronic P123 ratio of higher than 2 g/g. At higher than 3 g/g of TMP/Pluronic P123, excess TMP may form droplets in mixture and causes the constant pore diameter. At TMP/Pluronic P123 of higher than 3 g/g, surface area again increases to 1,100 m²/g. The pore diameter and surface area are increased with an addition of the hydrophobic TMP in the reaction gel because the hydrophobic TMP can penetrate into the hydrophobic region of the micelles and causes an expansion of hydrophobic core of micelles.

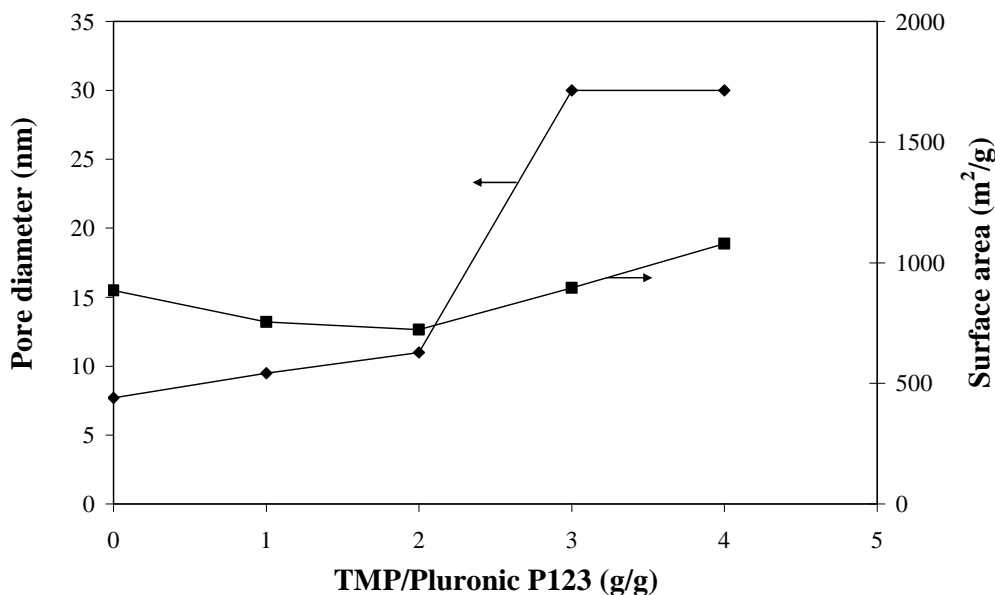


Figure 31 Effects of 2,3,4-trimethylpentane (TMP) on pore diameter and surface area of SBA-15 mesoporous silica

4.3 Tetrahexylammonium bromide (THB) as swelling agent

Tetrahexylammonium bromide has hardly affected the pore diameter of SBA-15 product. Maximum pore diameter of SBA-15 product obtained with THB as shown in Figure 32 is 7.9 nm. Pore diameter slowly decreases from 7.9 to 4.9 nm. Moreover, surface area also decreases from 885 to 346 m²/g when increasing the amount of THB. Therefore, it can be concluded that THB can not enhance the pore size of SBA-15 product. Because THB is considered as the hydrophilic substance since it can not penetrate into the hydrophobic cores of the micelles but disturbs the micelles formation. From this reason, pore diameter and surface area are decreased with increasing amount of THB. That is in good agreement with Nanta-ngern (2005), who studied the synthesis of mesoporous silica support from rice husk ash using 1-octanol as the hydrophilic swelling agent to expand the pore diameter and found that 1-octanol can not enhance the pore diameter.

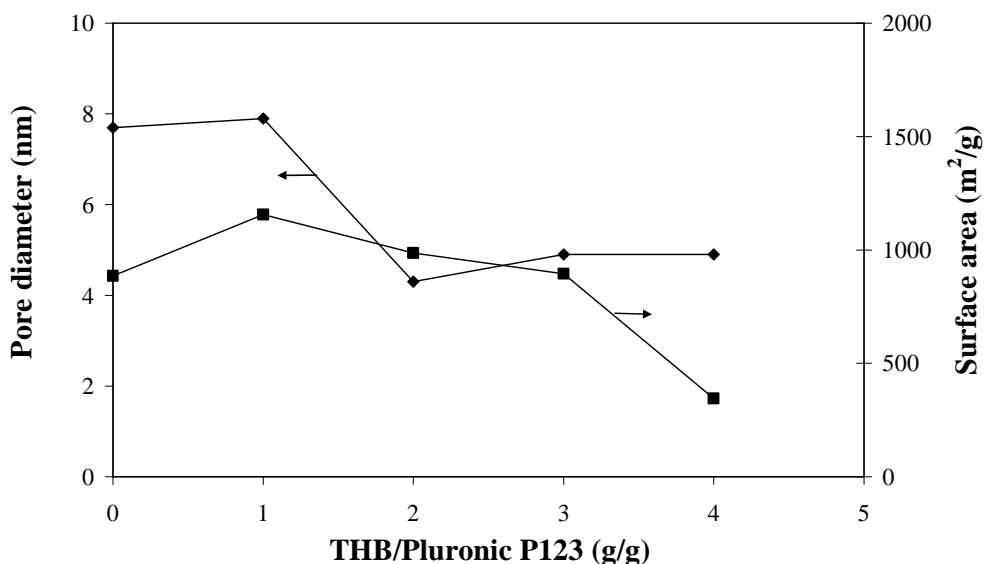


Figure 32 Effects of tetrahexylammonium bromide (THB) on pore diameter and surface area of SBA-15 mesoporous silica

4.4 N, N-dimethyldecylamine (DMD) as swelling agent

In the case of N, N-dimethyldecylamine as shown in Figure 33, we found that pore diameter decreases with increasing amount of DMD from 0-4 g/g. In contrast, surface area is hardly changed when increasing DMD/Pluronic P123 from 0-4 g/g, it increases only from 885 to 1,002 m²/g. Therefore, it can be concluded that DMD can not enhance the pore size of SBA-15 product. DMD is considered as a hydrophilic substance because it can dissolve within PEO block and /or water. From this reason, DMD has hardly affected the pore size of SBA-15 mesoporous silica.

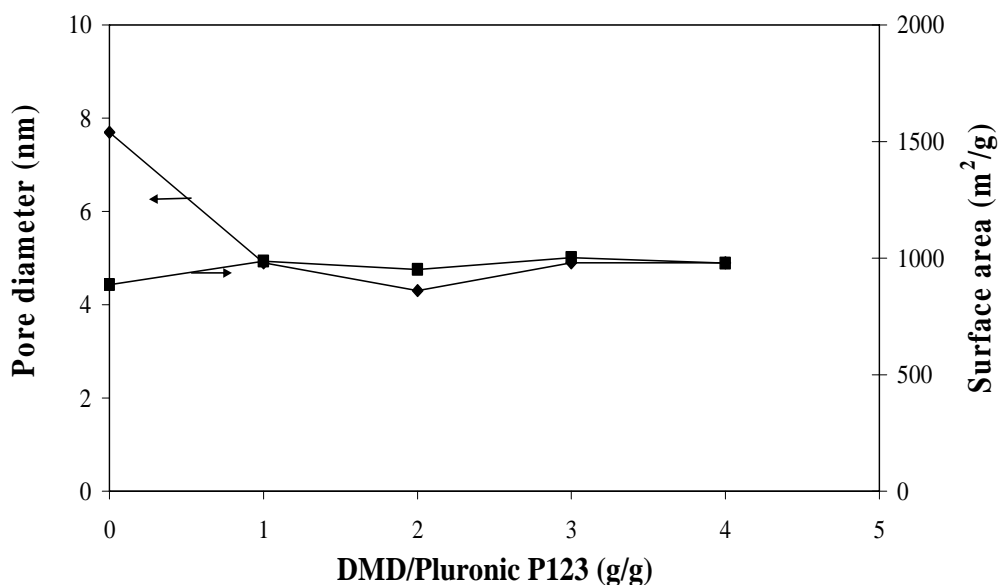


Figure 33 Effects of N, N-dimethyldecylamine (DMD) on pore diameter and surface area of SBA-15 mesoporous silica

According with the results of pore diameters and surface areas in Figures 30-33, the X-ray diffraction patterns of SBA-15 mesoporous silica prepared without and with using swelling agents are shown in Figure 34. The [100], [110] and [200] diffraction peaks, in this case, reveal the well-ordered hexagonal structure. SBA-15 mesoporous silica obtained from without using swelling agent shows an ordered hexagonal of SBA-15 mesoporous silica of which the complete small angle diffraction peaks at [100], [110] and [200] are clearly observed. In contrast, the

mesoporous silica products obtained with using swelling agent show disordered hexagonal structure as can be seen the disappearance of those small angle diffraction peaks. It may be occurred from the swelling agents as hydrophobic organic species adding to the reaction gel that was roughly penetrated into the hydrophobic region of the micelles, causing the disordered hexagonal structure. The result is similar to that of Jana *et al.* (2004), who studied the pore size control of mesoporous molecular sieves using different organic auxiliary chemicals. They found that XRD patterns of SBA-15s prepared by using methyl-substituted benzene, isopropyl-substituted benzene showed disordered hexagonal structure.

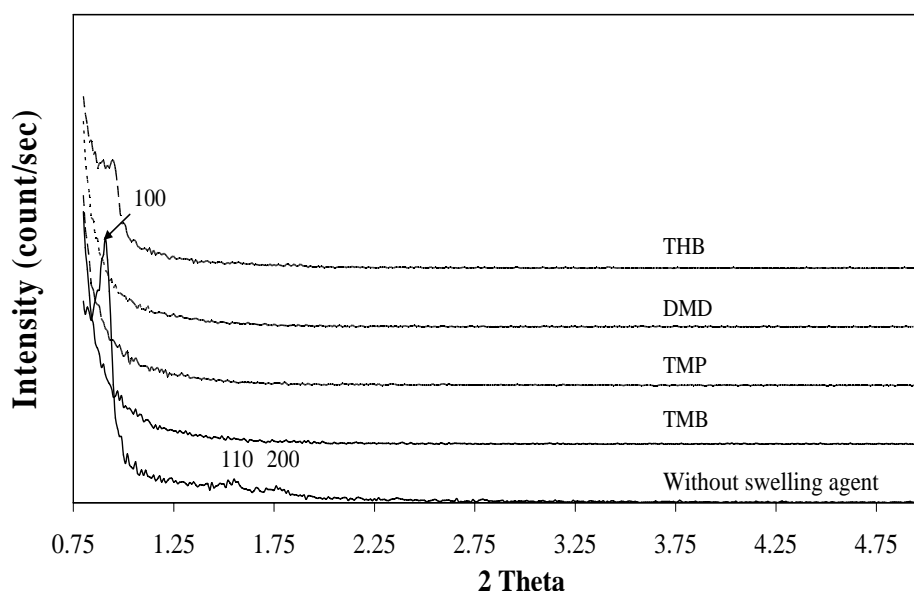


Figure 34 X-ray diffraction patterns of mesoporous silicas prepared without and with using swelling agents

5. Formation mechanism of SBA-15 mesoporous silica

In this part, the formation mechanisms of SBA-15 mesoporous silica with the addition of various types of swelling agents were proposed. The swelling agents such as TMB, TMP, THB and DMD have different types of the structure, resulting in the different degrees of polarity among these swelling agents. The swelling agents used in this research were divided into two types as follows: 1) hydrophobic molecules

such as TMB and TMP and 2) less hydrophobic molecules such as THB and DMD. Thus, the formation mechanisms of SBA-15 mesoporous silicas obtained from these hydrophobic and less hydrophobic molecules were discussed below.

5.1 Hydrophobic molecules: TMB and TMP

The formation of SBA-15 with swelling agents TMB and TMP are step-by-step proposed as follows:

a) The formation of Pluronic P123 micelles in aqueous solution is due to their self assemble properties of Pluronic P123 of which can be divided as two parts, polyethylene oxide (PEO) and polypropylene oxide (PPO) parts. PEO is a strong hydrophilic (water loving) moiety and PPO is a strong hydrophobic (water fearing) moiety.

b) The micelles start the growth process and become elongated, which composed of spherical and elongated micelles.

c) When adding hydrophobic TMB and TMP in the micelles, the hydrophobic TMB and TMP can penetrate into the hydrophobic cores of the micelles. This causes an expansion of the hydrophobic cores of micelles.

d) After the addition of micelles into P123 solution, sodium silicate as the silica source is added into the mixture. Silicas in the form of silanol groups then start to polymerize as the silica network by the linkages between silanol groups (Si-OH) and cover up the swelled Pluronic P123 micelles. The formation of the inorganic-organic composites is based on H-bonding between the surfactant and the silanol groups in the system.

The possible formation mechanism of SBA-15 mesoporous silica with TMB and TMP is shown as the schematic diagram in Figure 35.

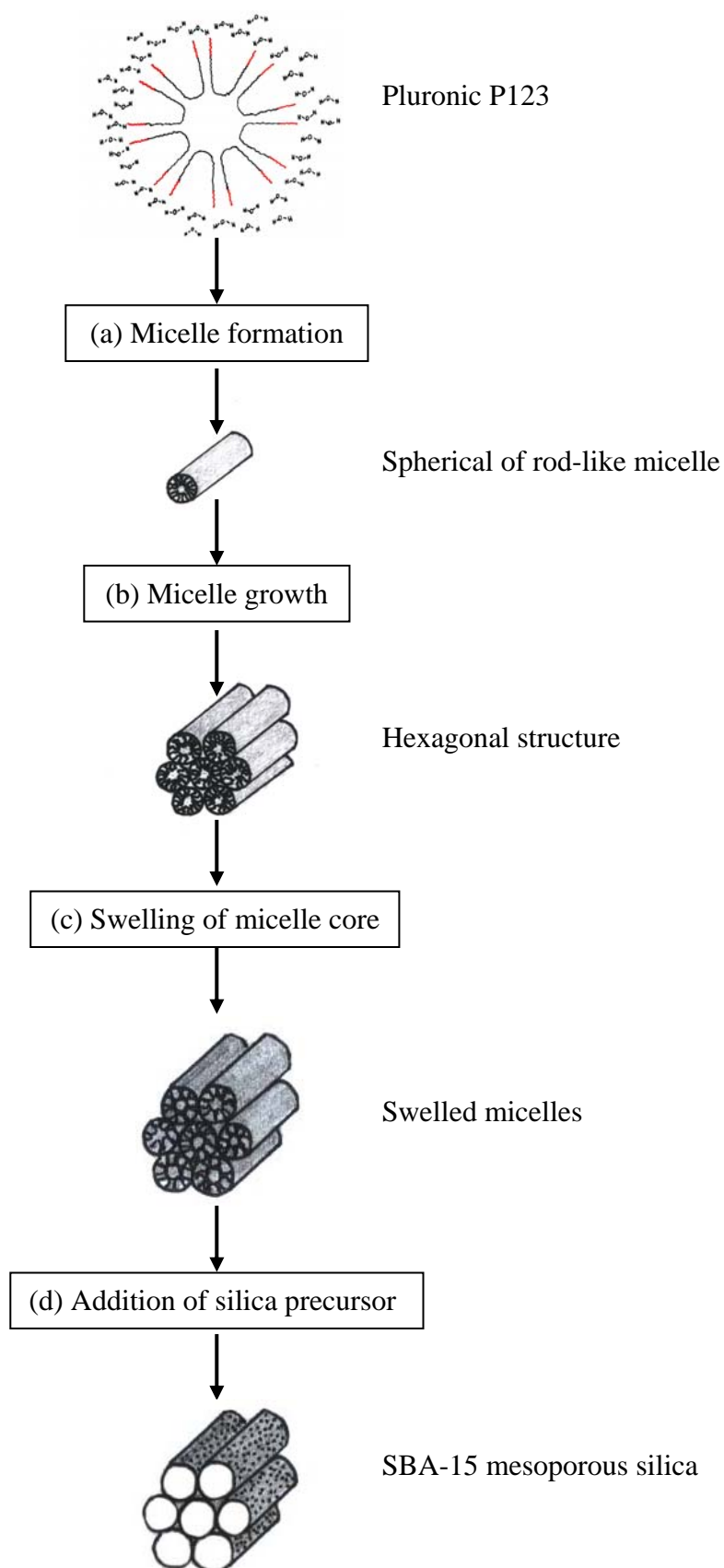


Figure 35 The formation mechanism of SBA-15 with swelling agent

The pore diameter is increased with the addition of the hydrophobic TMB and TMP in the reaction gel, the hydrophobic TMB and TMP can easily penetrate into the hydrophobic cores of the micelles. This causes an expansion of hydrophobic cores of micelles from 7.7 to 30 nm. With TMB, the micelles diameter increase more than that of TMP because TMB has flat coin shape, it can penetrate into the hydrophobic cores of the micelles while TMP has the branch chain shape of which can also penetrate and insert between the hydrophobic region and cause minor change of the pore diameter. The structures of TMB and TMP are shown in Figure 36. Swelled micelles with TMB and TMP are illustrated as the schematic diagrams shown in Figures 37 and 38, respectively.

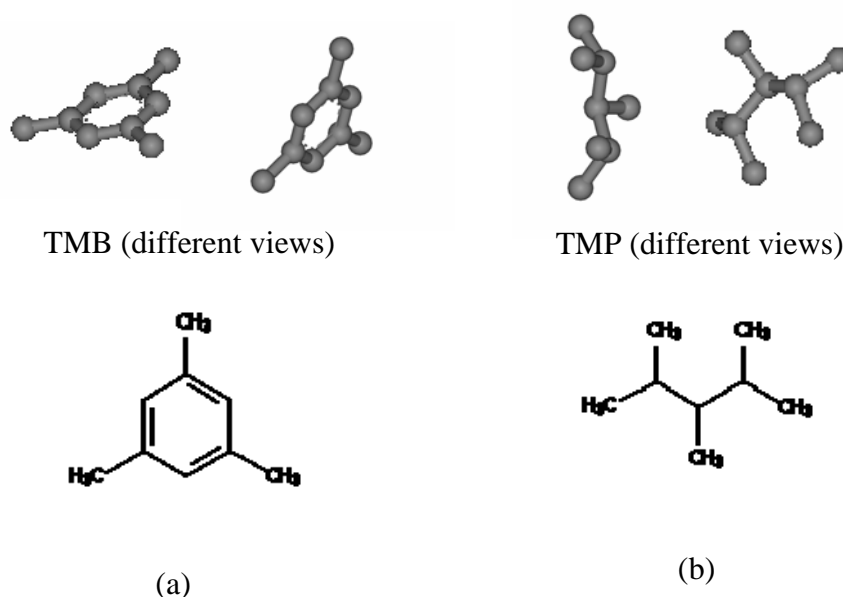


Figure 36 The structures and schematic drawings of (a) 1,3,5-trimethylbenzene (TMB) and (b) 2,3,4-trimethylpentane (TMP)

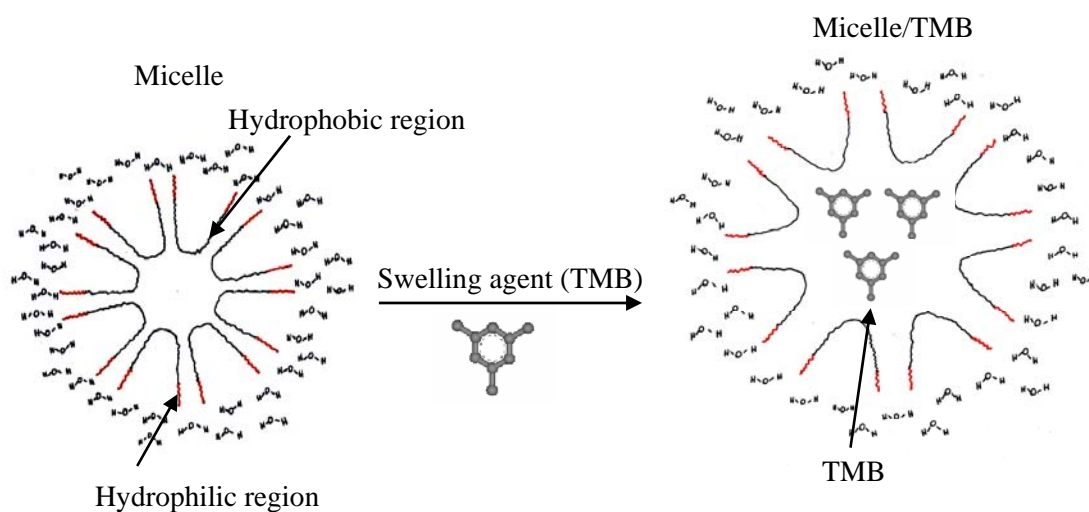


Figure 37 The expansion of micelle with 1,3,5-trimethylbenzene (TMB) as swelling agent

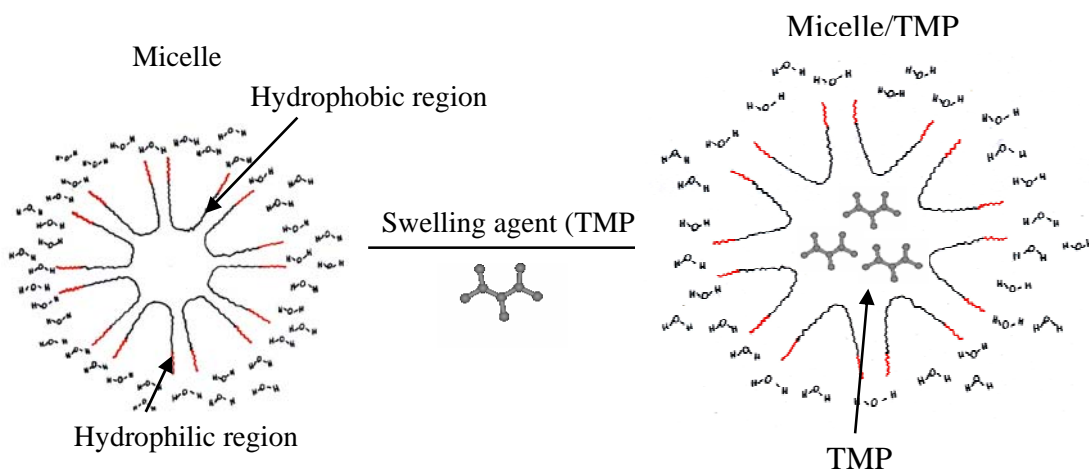


Figure 38 The expansion of micelle with 2,3,4-trimethylpentane (TMP) as swelling agent

5.2 Less hydrophobic molecules: THB and DMD

In this case, the formation mechanisms are similar in the stages of micelle formation (a), micelle growth (b) and the addition of silica precursor (d). This is because the less-hydrophobic substances such as tetrahexylammonium bromide (THB) and N,N-dimethyldecylamine (DMD) compose of hydrophobic and hydrophilic parts. Hexyl group is the hydrophobic part of THB, this part can penetrate into the hydrophobic cores of the micelles, whereas ammonium ion group is the hydrophilic part of THB which can penetrate into the water. In the case of DMD, amine group is the hydrophilic part and decyl group is the hydrophobic part. Structures of THB and DMD as swelling agents are shown in Figure 39.

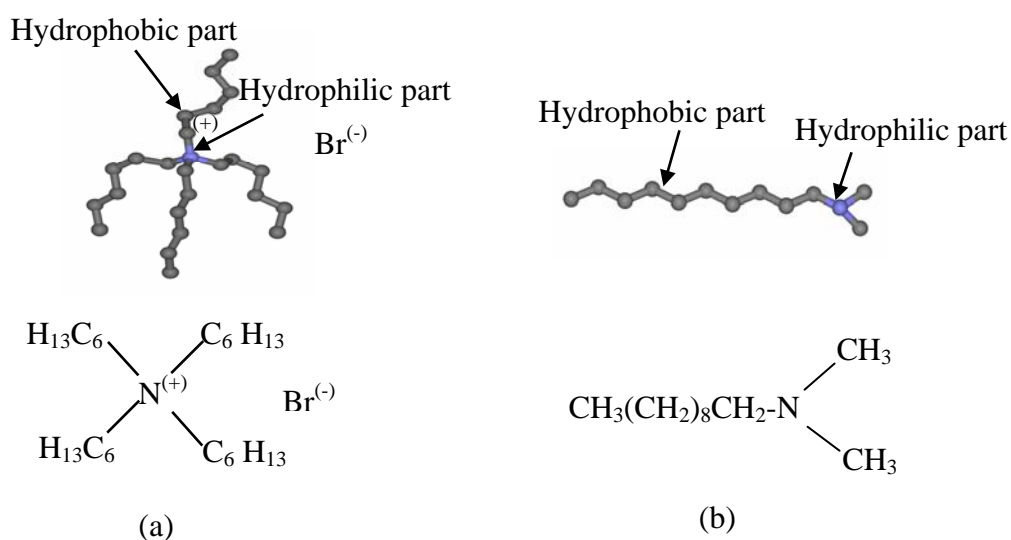


Figure 39 The structures and schematic drawings of (a) tetrahexylammonium bromide (THB) and (b) N, N-dimethyldecylamine (DMD)

Pore diameters decrease with increasing the amount of THB or DMD as swelling agents. It may be explained as follows.

For THB as swelling agent, THB of which is composed of hydrophobic and hydrophilic parts and has trigonal pyramidal shape as shown in Figure 39. From the stage swelling of micelle core (c) as shown in Figure 35, when THB was added,

the hydrophilic parts of THB then penetrate into the hydrophilic region of the micelles and then the micelles are pushed to shrink in order that the micelles and molecule of THB are in stable condition. This phenomena causes each micelles a little contraction and results as the decreasing of the pore diameter as the scheme shown in Figure 40.

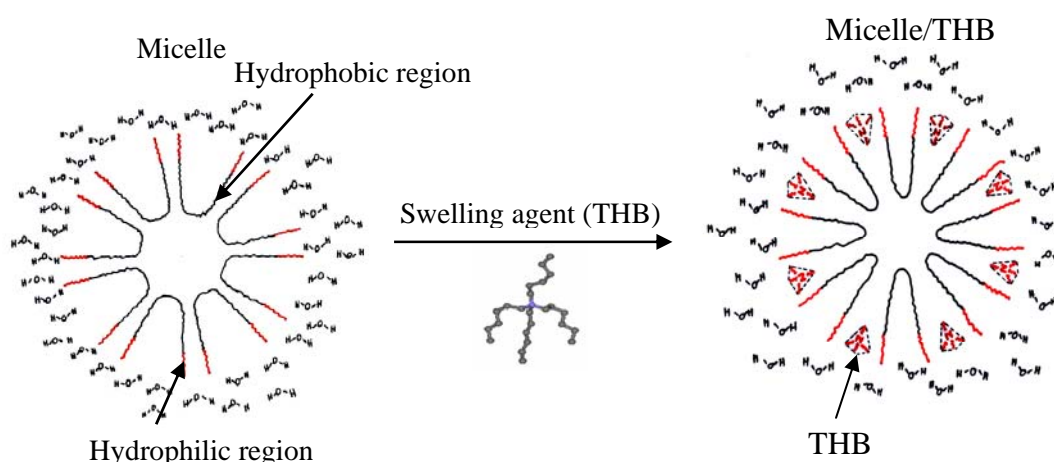


Figure 40 Shrinking micelle with tetrahexylammonium bromide (THB) as swelling agent.

When DMD as less hydrophobic molecules were added into the micelles, the hydrophobic parts of DMD penetrate into the hydrophobic regions of the micelles while the hydrophilic parts of these molecules penetrate into the hydrophilic regions of the micelles. Similar to THB the micelles then move closer and shrink to the more stable size. From this reason, this causes the decreasing of the pore diameter as shown in Figure 41.

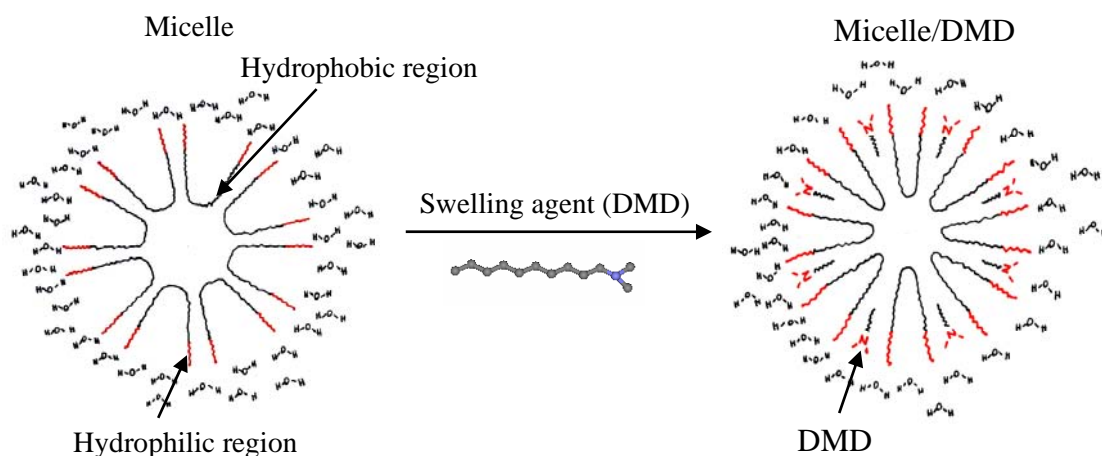


Figure 41 Shrinking of micelle with N,N-dimethyldecylamine (DMD) as swelling agent

CONCLUSIONS

The modification of pore diameter of SBA-15 mesoporous silica produced from rice husk ash by using swelling agents and operating condition including hydrolysis-condensation temperature, hydrothermal treatment temperature and amount of hydrochloric acid were investigated. The results can be concluded as follows:

The hydrolysis-condensation temperature of 35°C and hydrothermal treatment temperature of 110°C are the optimum synthesis temperatures. The oval-like shape SBA-15 obtained from this condition exhibits pore diameter of 7.7 nm, high surface area of 885 m²/g, total pore volume of 0.31 cm³/g and well-ordered hexagonal pore structure.

The effects of swelling agents for expanding and controlling the pore diameter of SBA-15 were investigated. The pore diameter can be expanded and controlled by using TMB and TMP as swelling agents. The maximum pore diameter of SBA-15 products is approximately 31 nm when TMB was used as swelling agent. In contrast, THB and DMD can not control the pore diameter of SBA-15 products. However, the SBA-15 mesoporous silica products obtained with using swelling agent show disordered hexagonal pore structure.

LITERATURE CITED

- Beck, J.S., J.C. Vartuli, W.J. Roth, M.E. Leonowicz, C.T. Kresge, K.D. Schmitt, C.T.W. Chu, D.H. Olson and E.W. Sheppard. 1992. A new family of mesoporous molecular sieves prepared with liquid crystal templates. **Journal of the American Chemical Society**. 114: 10834-10843.
- Boissiere, C., A. Larbot, A. van der Lee, P.J. Kooyman and E. Prouzet. 2000. A new synthesis of mesoporous silica MSU-X controlled by a two-step pathway. **Chemistry of Materials**. 12: 2902-2913
- Berggren, A., A.E.C. Palmqvist and K. Holmberg. 2005. Surfactant-templated mesostructured materials from inorganic silica. **Soft Matter**. 1: 219-226.
- Blin, J.L., C. Otjacques, G. Herrier and B. Su. 2000. Pore size engineering of mesoporous silicas using decane as expander. **Langmuir**. 16: 4229-4236.
- Chareonpanich, M., T. Namto, P. Kongkachuichay and J. Limtrakul. 2004. Synthesis of ZSM-5 zeolite from lignite fly ash and rice husk ash. **Fuel Processing Technology**. 85: 1623–1634.
- Choi, D.G and S.M. Yang. 2003. Effect of two-step sol–gel reaction on the mesoporous silica. **Journal of Colloid and Interface Science**. 261: 127-132.
- Ciesla, U. and F. Schüth. 1999. Ordered mesoporous materials. **Microporous and Mesoporous Materials**. 27: 131–149.
- Corma, A., A. Martínez and V. Martínez-Soria. 1997. Hydrogenation of aromatics in diesel fuels on Pt/MCM-41 catalysts. **Journal of Catalysis**. 169: 480-489.

- Corriu, R.J.P., A. Mehdi, C. Reyé and C. Thieuleux. 2004. Direct syntheses of functionalized mesostructured silica by using an inexpensive silica source. **Chem. Commun.** 1440-1441.
- Flodstrom, K and V. Alfredsson. 2003. Influence of the block length of triblock copolymers on the formation of mesoporous silica. **Microporous and Mesoporous Materials.** 59: 167–176.
- _____, H. Wenerstrom and V. Alfredsson. 2004. Mechanism of mesoporous silica formation, a time-resolved NMR and TEM study of silica-block copolymer aggregation. **Langmuir.** 20: 680-688.
- Hanyotee, S. 2004. **Synthesis of high purity ZSM-5 zeolite from lignite fly ash and silica from rice husk ash.** M.S. thesis, Kasetsart University.
- Harold, H.K and I.K. Edmond. 1996. Preparation of oxide catalysts and catalyst supports-a review of recent advances. **The Chemical Engineering Journal.** 64: 203-214.
- Jana, S.K., R. Nishida, K. Shindo, T. Kugita and S. Namba. 2004. Pore size control of mesoporous molecular sieves using different organic auxiliary chemicals. **Microporous and Mesoporous Materials.** 68: 133-142.
- Khodakov, A.Y., A. Griboval-Constant, R. Bechara and V.L. Zholobenko. 2002. Pore size effect in Fischer–Tropsch synthesis over cobalt-supported mesoporous silica. **Journal of Catalysis.** 206: 230-241.
- _____, _____ and R. Bechara. 2002. Fischer–Tropsch synthesis over silica supported cobalt catalyst: mesoporous structure versus cobalt surface density. **Applied Catalysis.** 254: 273-288.

- Kleitz, F., D. Liu, G.M. Anilkumar, I.S. Park, L.A. Solovyov, A.N. Shmakov and R. Ryoo. 2003. Large cage face-centered-cubic *Fm3m* mesoporous silica: synthesis and structure. **Journal of Physical Chemistry**. 107: 14296-14300.
- Kung, H.H and E.I. Ko. 1996. Preparation of oxide catalysts and catalyst supports-a review of recent advances. **The Chemical Engineering Journal**. 64: 203-214
- Kruk, M., M. Jaroniec and A. Sayari. 2000. New insights into pore size expansion of mesoporous silicates using long chain amines. **Microporous and Mesoporous Materials**. 35-36: 545-553.
- Lettow, J.S., Y.J. Han, P. Schmidt-Winkel, P. Yang, D. Zhao, G.D. Stucky and J.Y. Ying. 2000. Hexagonal to mesocellular foam phase transition in polymer-templated mesoporous silicas. **Langmuir**. 16: 8291-8295.
- Li, W., Y. Yao, Z. Wang, J. Zhao, M. Zhao and C. Sun. 2001. Preparation of stable mesoporous silica FSM-16 from water glass in the presence of cetylpyridium bromide. **Materials Chemistry and Physics**. 70: 144-149.
- Linssen, T., K. Cassiers, P. Cool and E.F. Vansant. 2003. Mesoporous templated silicates: an overview of their synthesis, catalytic activation and evaluation of the stability. **Advances in Colloid and Interface Science**. 103: 121-147.
- Luechinger, M., G.D. Pirngruber, B. Lindlar, P. Lagner and R. Prins. 2005. The effect of the hydrophobicity of aromatic swelling agents on pore size and shape of mesoporous silicas. **Microporous and Mesoporous Materials**. 79: 41-52.
- Marczewska, D.A., A.W. Marczewski, I. Skrzypek, S. Pikus and M. Kozak. 2005. The effect of aging temperature on structure characteristics of ordered mesoporous silicas. **Applied Surface Science**. 252: 625-632.

- Martines, M.A.U., E. Yeong, A. Larbot and E. Prouzet. 2004 Temperature dependence in the synthesis of hexagonal MSU-3 type mesoporous silica synthesized with Pluronic P123 block copolymer. **Microporous and mesoporous Materials**. 74: 213-220.
- Mou, C.Y and H.P. Lin. 2000. Control of morphology in synthesizing mesoporous silica. **Pure and Applied Chemistry**. 72: 137–146.
- Nanta-ngern, A. 2005. **The synthesis of mesoporous silica support from rice husk ash**. M.S. thesis, Kasetsart University.
- Ohtsuka, Y. 2002. Utilization of cobalt catalysts supported on mesoporous silica for efficient production of diesel fuels by FT synthesis. **Fuel and Energy Abstracts**. 44: 213.
- _____, Y. Wang, M. Noguchi and Y. Takahashi. 2001. Synthesis of SBA-15 with different pore sizes and the utilization as supports of high loading of cobalt catalysts. **Catalysis Today**. 68: 3-9.
- _____, Y. Takahashi, M. Noguchi, T. Arai, S. Takasaki, N. Tsubouchi and Y. Wang. 2004. Novel utilization of mesoporous molecular sieves as supports of cobalt catalysts in Fischer–Tropsch synthesis. **Catalysis Today**. 89:419-429.
- _____, A.S. Bagshaw and E. Prouzet. 1995. Templating of mesoporous molecular sieves by nonionic polyethylene oxide surfactants. **Science**. 269: 1242-1244.
- Panpranot, J., J.J.G. Goodwin and A. Sayari. 2002. Synthesis and characteristics of MCM-41 supported Co-Ru catalysts. **Catalysis Today**. 77: 269-284.

- Pei, Lihua., K. Kurumada, M. Tanigaki, M. Hiro and K. Susa. 2004. Effect of drying on the mesoporous structure of sol-gel derived silica with PPO-PEO-PPO template block copolymer. **Journal of colloid Interface Science.** 284: 222-227
- Pinnavaia, T.J. and P. Tanev. 1995. A neutral templating route to mesoporous molecular sieves. **Science.** 267
- Ruthstein, S., J. Schmidt, E. Kesselman, Y. Talmon and D. Goldfarb. 2006. Resolving Intermediate Solution Structures during the Formation of Mesoporous SBA-15. **Journal of the American Chemical Society.**128:3366-3374.
- Schmidt-Winkel, P., W.W. Lukens, Jr. Peidong Yang, D.I. Margolese, J.S. Lettow, J.Y. Ying and G.D. Stucky. 1999. Microemulsion templating of siliceous mesostructured cellular foams with well-defined ultralarge mesopores. **Chemistry of Materials.** 12: 686-696
- Selvam, P., S.K. Bhatia and C.G. Sonwane. 2001. Recent advances in processing and characterization of periodic mesoporous MCM-41 silicate molecular sieves. **Industrial Engineering Chemistry Research.** 40: 3237-3261
- Sing, K.S.W., D.H. Everett, R.A.W. Haul, L. Moscou, R.A. Pierotti, J. Rouquerol and T. Siemieniewska. 1985. Reporting physisorption data for gas/solid systems with special reference to the determination of surface area and porosity. **International Union of Pure and Applied Chemistry.** 57: 603-619.
- Soler-Illia, G.J., A.A De, E.L. Crepaldi, D. Grosso and C. Sanchez. 2003. Block copolymer-templated mesoporous oxides. **Current Opinion in Colloid & Interface Science.** 8 (1): 109-126.

- _____, E.L. Crepaldi, D. Grosso and C. Sanchez. 2003. Block copolymer-templated mesoporous oxides. **Colloid and Interface Science**. 8: 109–126
- Tendeloo, G.V., W.J.J. Stevens, M. Mertens, S. Mullens, I. Thijs, P. Cool and E.F. Vansant. 2006. Formation mechanism of SBA-16 spheres and control of their dimensions. **Microporous and Mesoporous Materials**. 119–124,
- Vannice, M.A. 1977. The catalytic synthesis of hydrocarbons from H₂/CO mixtures over the Group VIII metals: V. The catalytic behavior of silica-supported metals. **Journal of Catalysis**. 50: 228-236.
- Wang, Y., M. Noguchi, Y. Takahashi and Y. Ohtsuka. 2001. Synthesis of SBA-15 with different pore sizes and utilization as supports of high loading of cobalt catalysts. **Catalysis Today**. 68: 3-9.
- Xia, Y., R. Mokaya and J. J. Titman. 2004. Formation of molecularly ordered layered mesoporous silica via phase transformation of silicate-surfactant composites. **Journal of Physical Chemistry**. 108(31): 11361 – 11367.
- Yin, D., W. Li, W. Yang, H. Xiang, Y. Sun, B. Zhong and S. Peng. 2001. Mesoporous HMS molecular sieves supported cobalt catalysts for Fischer–Tropsch synthesis. **Microporous and Mesoporous Materials**. 47: 15-24.
- Zhao, D., J. Feng, Q. Huo and N. Melosh. 1998. Triblock copolymer syntheses of mesoporous silica with periodic 50 to 300 angstrom pores. **Science**. 279: 548-552
- _____, J. Sun, Q. Li and G.D. Stucky. 2000. Morphological control of highly ordered mesoporous silica SBA-15. **Chemistry of Materials**. 12: 275-279.

Zhao, D., Q. Huo, J. Feng, B.F. Chmelka and G.D. Stucky. 1998. Nonionic triblock and star diblock copolymer and oligomeric surfactant syntheses of highly ordered, hydrothermally stable, mesoporous silica structures. **Journal of the American Chemical Society.** 120: 6024-6036.

Department of energy business. 2005. **Static data of fuel.** Available source: http://www.doeb.go.th/information/infor_conclude.html, December 12, 2005.

Sigma-Aldrich. 2006. **Physical properties of swelling agents.** Available source: <https://www.sigmaaldrich.com/catalog/search/ProductDetail/FLUKA/92613>, June 13, 2006.

Chemat Technology. 2005. **The sol-gel process for the silica network preparation.** Available source: <http://www.chemat.com/html/solgel.html>, November 25, 2004.

University of Calgary. 2005. **Micellization of surfactant in aqueous solution.** Available source: <http://www.ucalgary.ca/UofC/faculties/SC/SC.html>, December 12, 2005.

APPENDIX

Appendix A

Design of Experiment for Synthesis of SBA-15 Mesoporous Silica

Design of Experiment (DOE)

The effect of operating conditions including hydrolysis-condensation temperature, hydrothermal treatment temperature, amount of hydrochloric acid and swelling agents on the properties of SBA-15 materials were considered. Design of Experiment (DOE) method was used to study relation of these factors on the properties of SBA-15 mesoporous silica. The detail conditions for DOE study were as follows: hydrolysis-condensation temperature, 30-50°C; hydrothermal treatment temperature, 90-120°C; amounts of HCl and TMB as swelling agent, 3-5 M and 0.5-4 g/g of TMB/Pluronic P123, respectively. Factorial design of 4 factors was applied. Higher and lower values of each factor were used in 2^k factorial design method. Consequently, all experiments are designed as 16 batches for checking the interaction of these factors.

Effect between each factor and interaction on pore size and surface area were calculated by Equation (A1).

$$\text{Factor effect} = \frac{1}{2^{k-1} \cdot n} \cdot (\text{contrast}) \quad (\text{A1})$$

Where k is amount of factor
 n is amount of repeated experiment

Affecting the pore size and surface area are plotted between % normal probability and effect as shown in example of experiment design.

Example of experimental design

Appendix Table A1 Boundary values of each factor for synthesizing SBA-15 mesoporous silica

Factors ¹	Factor levels	
	Low (-)	High (+)
A	30	50
B	90	120
C	3	5
D	0.5	3

¹ A= Hydrolysis-condensation temperature, B=Hydrothermal treatment temperature, C=Amount of hydrochloric acid and D=Amount of swelling agent

Appendix Table A2 Effect of each factor on surface area and pore size of SBA-15 mesoporous silica

Run No.	Factor Effect ¹				Surface area (m ² /g)	Pore size (nm)	Treatment combination
	A	B	C	D			
1	-	-	-	-	675	17.3	(1)
2	+	-	-	-	705	17.5	A
3	-	+	-	-	647	30.5	B
4	+	+	-	-	647	31.4	AB
5	-	-	+	-	673	17.3	C
6	+	-	+	-	570	17.5	AC
7	-	+	+	-	516	30.5	BC
8	+	+	+	-	820	17.3	ABC
9	-	-	-	+	406	29.9	D
10	+	-	-	+	539	17.3	AD
11	-	+	-	+	455	30.5	BD
12	+	+	-	+	605	30.7	ABD
13	-	-	+	+	692	17.3	CD
14	+	-	+	+	589	17.3	ACD
15	-	+	+	+	641	17.3	BCD
16	+	+	+	+	886	30.8	ABCD

¹ - = high boundary value of each factor

+ = low boundary value of each factor

Appendix Table A3 Contrast value in Equation (A1) for the 2^4 design

	A	B	AB	C	AC	BC	ABC	D	AD	BD	ABD	CD	ACD	BCD	ABCD
(1)	-	-	+	-	+	+	-	-	+	+	-	+	-	-	+
a	+	-	-	-	-	+	+	-	-	+	+	+	+	-	-
b	-	+	-	-	+	-	+	-	+	-	+	+	-	+	-
ab	+	+	+	-	-	-	-	-	-	-	-	+	+	+	+
c	-	-	+	+	-	-	+	-	+	+	-	-	+	+	-
ac	+	-	-	+	+	-	-	-	-	+	+	-	-	+	+
bc	-	+	-	+	-	+	-	-	+	-	+	-	+	-	+
abc	+	+	+	+	+	+	+	-	-	-	-	-	-	-	-
d	-	-	+	-	+	+	-	+	-	-	+	-	+	+	-
ad	+	-	-	-	-	+	+	+	+	-	-	-	-	+	+
bd	-	+	-	-	+	-	+	+	-	+	-	-	+	-	+
abd	+	+	+	-	-	-	-	+	+	+	+	-	-	-	-
cd	-	-	+	+	-	-	+	+	-	-	+	+	-	-	+
acd	+	-	-	+	+	-	-	+	+	-	-	+	+	-	-
bcd	-	+	-	+	-	+	-	+	-	+	-	+	-	+	-
abcd	+	+	+	+	+	+	+	+	+	+	+	+	+	+	+

To illustrate the use of Table A3, consider a 2^4 factorial design. The contrast for A and ABCD would be

$$\text{Contrast}_A = -(1)+a-b+ab-c+ac-bc+abc-d+ad-bd+abd-cd+acd-bcd+abcd$$

$$\text{Contrast}_{ABCD} = (1)-a-b+ab-c+ac+bc-abc-d+ad+bd-abd+cd-acd-bcd+abcd$$

Calculated results of contrast and factor effect values are shown in Table A4.

Appendix Table A4 Contrast and factor effect values for 2^4 factorial design on pore size and surface area of SBA-15 mesoporous silica

Model term	Pore size		Surface area	
	Factor effect	Contrast	Factor effect	Contrast
A	-1.35	-10.8	82	656
B	8.45	67.6	46	368
C	-4.975	-39.8	88.5	708
D	1.475	11.8	-55	-440
AB	1.7	13.6	92.75	742
AC	1.475	11.8	3.75	30
AD	1.625	13	24.25	194
BC	-1.825	-14.6	38.75	310
BD	-1.575	-12.6	44.25	354
CD	-1.45	-11.6	112.25	898
ABC	-1.675	-13.4	96	768
ABD	4.875	39	-1.5	-12
ACD	5	40	-39	-312
BCD	1.7	13.6	-6	-48
ABCD	1.85	14.8	-13.25	-106

Before starting plotted graph between % normal probability and factor effect, % normal probability can be calculated in Equation (A2).

$$\% \text{ Normal probability} = \left(\frac{j-0.5}{N} \right) \times 100 \quad (\text{A2})$$

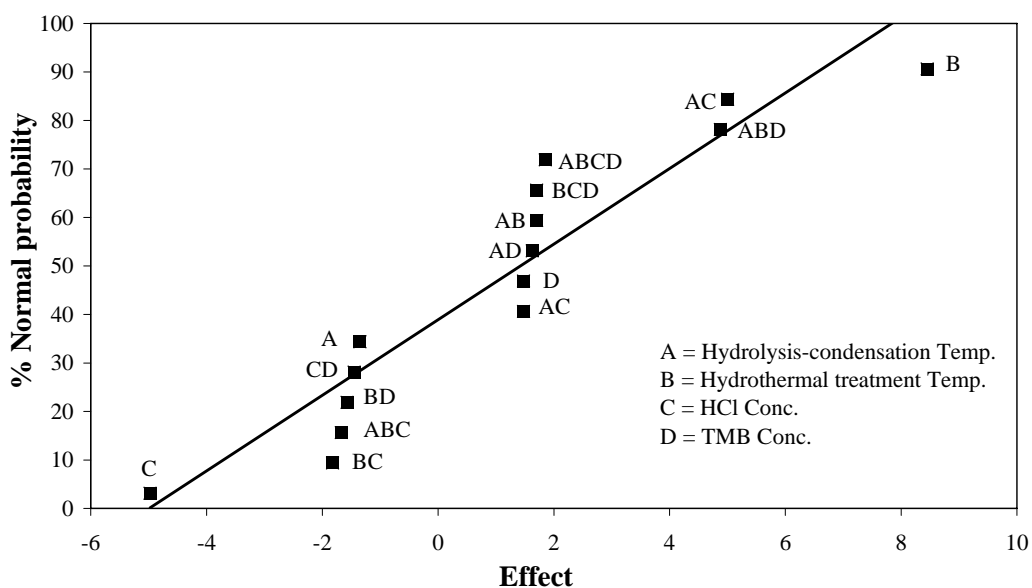
Where j is sequence of factor effect from low to high value

N is amount of net factor effect in all experiment

Appendix Table A5 The result of % normal probability on pore size of SBA-15 mesoporous silica

Sequence (j)	Model term	Factor effect	% Normal probability
1	C	-4.975	3.125
2	BC	-1.825	9.375
3	ABC	-1.675	15.625
4	BD	-1.575	21.875
5	CD	-1.45	28.125
6	A	-1.35	34.375
7	AC	1.475	40.625
8	D	1.475	46.875
9	AD	1.625	53.125
10	AB	1.7	59.375
11	BCD	1.7	65.625
12	ABCD	1.85	71.875
13	ABD	4.875	78.125
14	ACD	5	84.375
15	B	8.45	90.625

From Table A5 was plotted between % normal probability and factor effect as shown in Appendix Figure A1.



Appendix Figure A1 The relation of % normal probability and factor effect on pore size for synthesizing SBA-15 mesoporous silica

The pore size data is plotted between % normal probability and factor effect as shown in Appendix Figure A1. All of the effects that lie along the correlation line are negligible, whereas the significant effects are located far away from the correlation line.

Pore size data as shown in Appendix Figure A1 shows that the important effects obtained from this analysis are the significant effects as shown in the order of importance as follows: $A * B * C * D > B > B * C > B * C * D > A * B * C \gg$ others remaining effects.

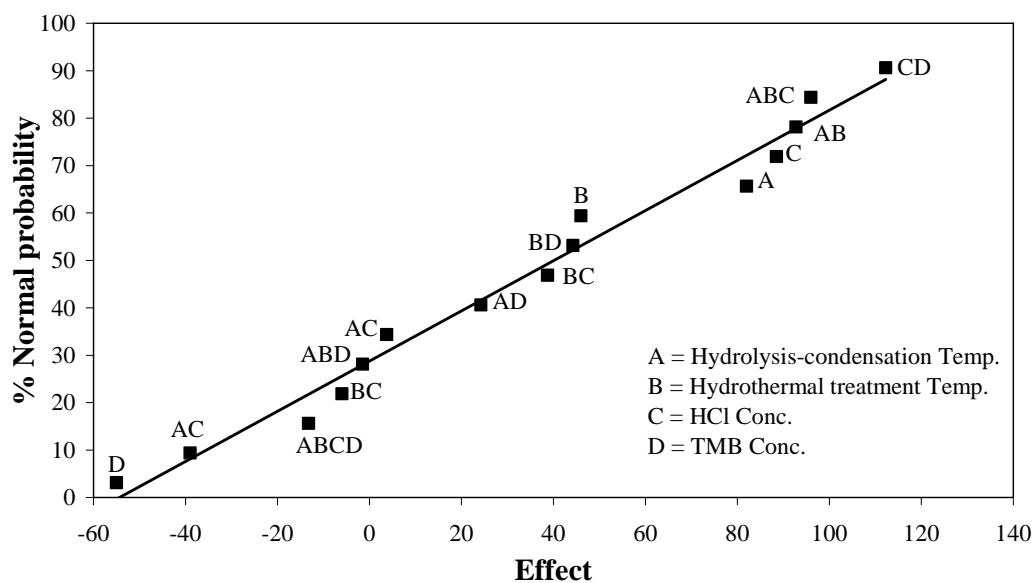
As the DOE results, effect of A, C, D and the other interactions can be neglected.

From this result, it indicates that all the factors including hydrolysis-condensation temperature (A), hydrothermal treatment temperature (B), amounts of HCl (C) and amounts of TMB (D) have significant effect on the pore size.

Appendix Table A6 The result of % normal probability on surface area of SBA-15 mesoporous silica

Sequence (j)	Model term	Factor effect	% Normal probability
1	D	-55	3.125
2	ACD	-39	9.375
3	ABCD	-13.25	15.625
4	BCD	-6	21.875
5	ABD	-1.5	28.125
6	AC	3.75	34.375
7	AD	24.25	40.625
8	BC	38.75	46.875
9	BD	44.25	53.125
10	B	46	59.375
11	A	82	65.625
12	C	88.5	71.875
13	AB	92.75	78.125
14	ABC	96	84.375
15	CD	112.25	90.625

From Table A6 was plotted between % normal probability and factor effect as shown in Appendix Figure A2.



Appendix Figure A2 The relation of % normal probability and factor effect on surface area for synthesizing SBA-15 mesoporous silica

For surface area data, we found that the important effects obtained from this analysis are as follows: A and B > A * B * C * D > A * B * C >> others remaining effects.

According to the observed pore size response and surface area response, the factors effect on the textural properties of SBA-15 are hydrolysis-condensation temperature (A), hydrothermal treatment temperature (B), amounts of HCl (C) and amounts of TMB (D).

Appendix Table A7 Synthesis temperature condition

Run No.	Temperature	
	Hydrolysis-condensation temperature (°C)	Hydrothermal treatment temperature (°C)
1	30	90
2	30	100
3	30	110
4	30	120
5	35	90
6	35	100
7	35	110
8	35	120
9	40	90
10	40	100
11	40	110
12	40	120
13	50	90
14	50	100
15	50	110
16	50	120

Appendix Table A3 Contrast value in Equation (A1) for the 2^4 design

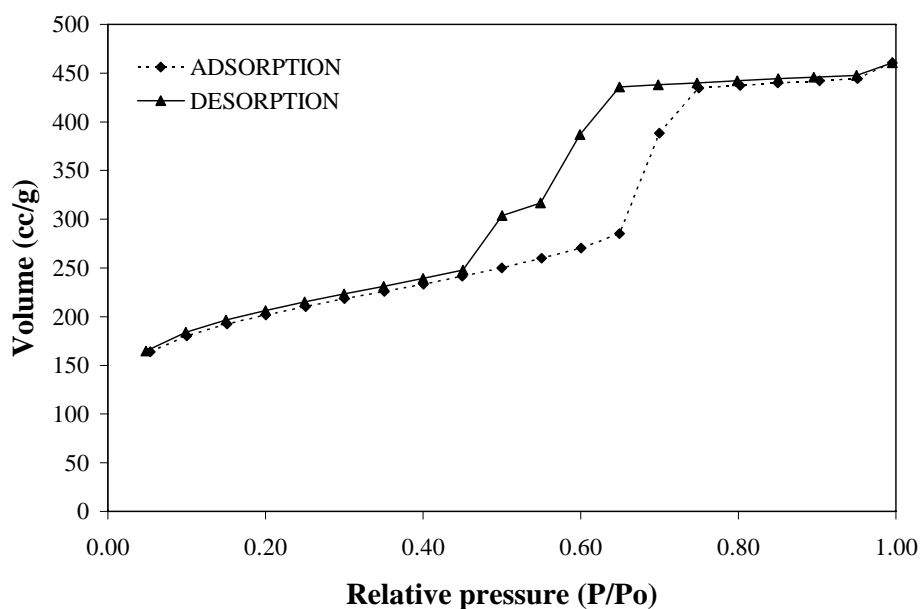
	A	B	AB	C	AC	BC	ABC	D	AD	BD	ABD	CD	ACD	BCD	ABCD
(1)	-	-	+	-	+	+	-	-	+	+	-	+	-	-	+
a	+	-	-	-	-	+	+	-	-	+	+	+	+	-	-
b	-	+	-	-	+	-	+	-	+	-	+	+	-	+	-
ab	+	+	+	-	-	-	-	-	-	-	-	+	+	+	+
c	-	-	+	+	-	-	+	-	+	+	-	-	+	+	-
ac	+	-	-	+	+	-	-	-	-	+	+	-	-	+	+
bc	-	+	-	+	-	+	-	-	+	-	+	-	+	-	+
abc	+	+	+	+	+	+	+	-	-	-	-	-	-	-	-
d	-	-	+	-	+	+	-	+	-	-	+	-	+	+	-
ad	+	-	-	-	-	+	+	+	+	-	-	-	-	+	+
bd	-	+	-	-	+	-	+	+	-	+	-	-	+	-	+
abd	+	+	+	-	-	-	-	+	+	+	+	-	-	-	-
cd	-	-	+	+	-	-	+	+	-	-	+	+	-	-	+
acd	+	-	-	+	+	-	-	+	+	-	-	+	+	-	-
bcd	-	+	-	+	-	+	-	+	-	+	-	+	-	+	-
abcd	+	+	+	+	+	+	+	+	+	+	+	+	+	+	+

Appendix B

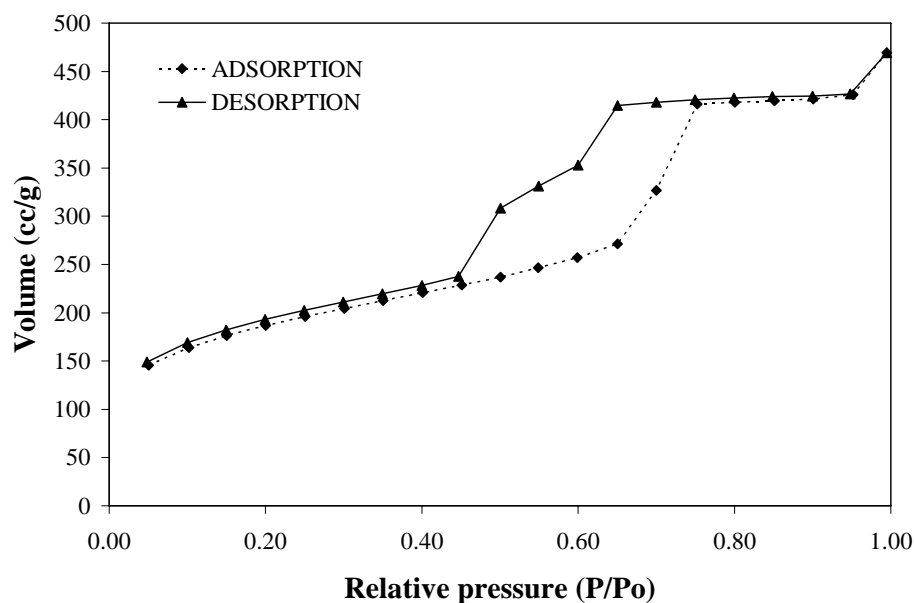
Autosorb-1 Analyzer Data

Adsorption-Desorption Isotherm

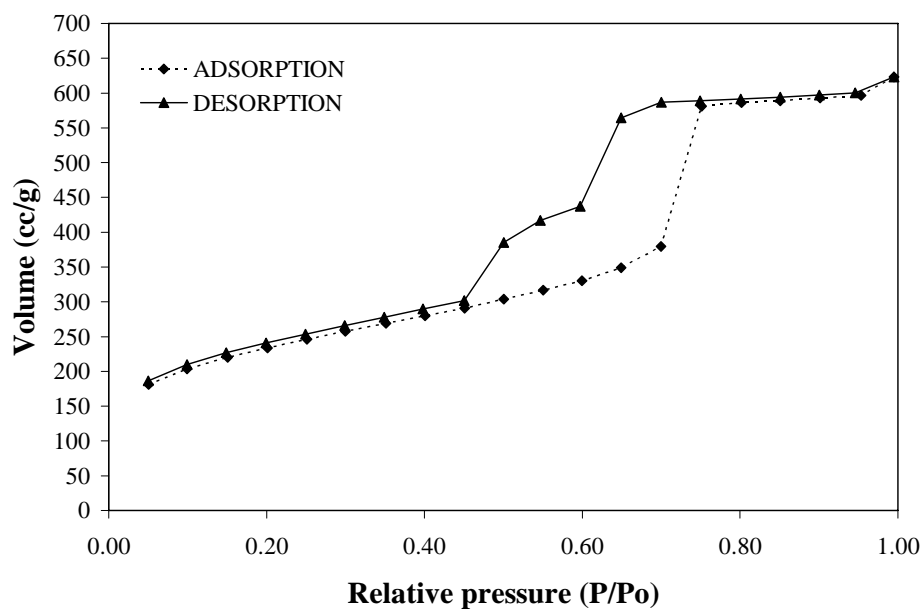
Appendix Figures B1-B16 show the sorption isotherms of synthesized SBA-15 mesoporous silica at various hydrolysis-condensation temperatures of 30, 35, 40 and 50°C and hydrothermal treatment temperatures of 90, 100, 110 and 120°C. Both reaction periods were fixed at 24 h, for surface area, total pore volume and pore size are shown in Table B1.



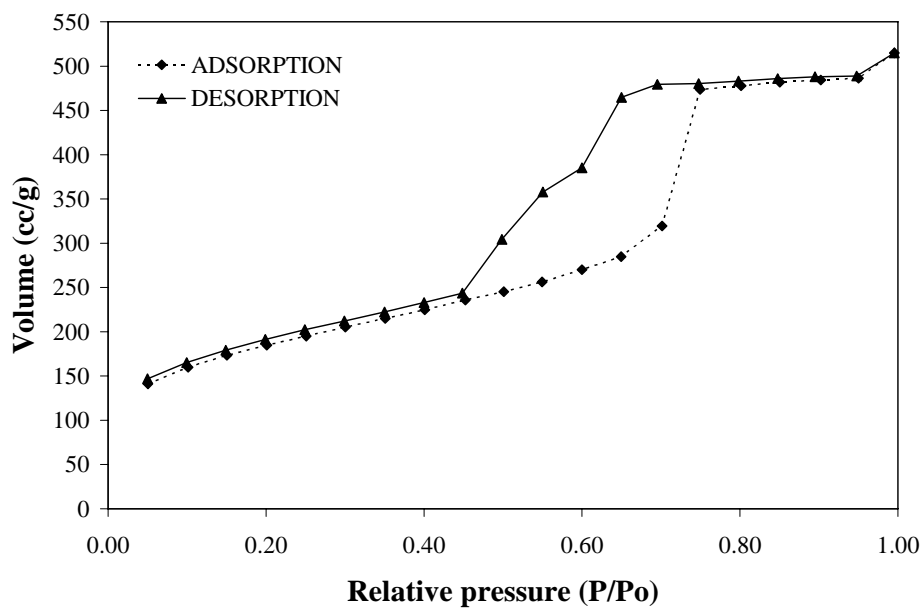
Appendix Figure B1 Sorption isotherm of SBA-15 product at hydrolysis-condensation temperature of 30°C and hydrothermal treatment temperature of 90°C



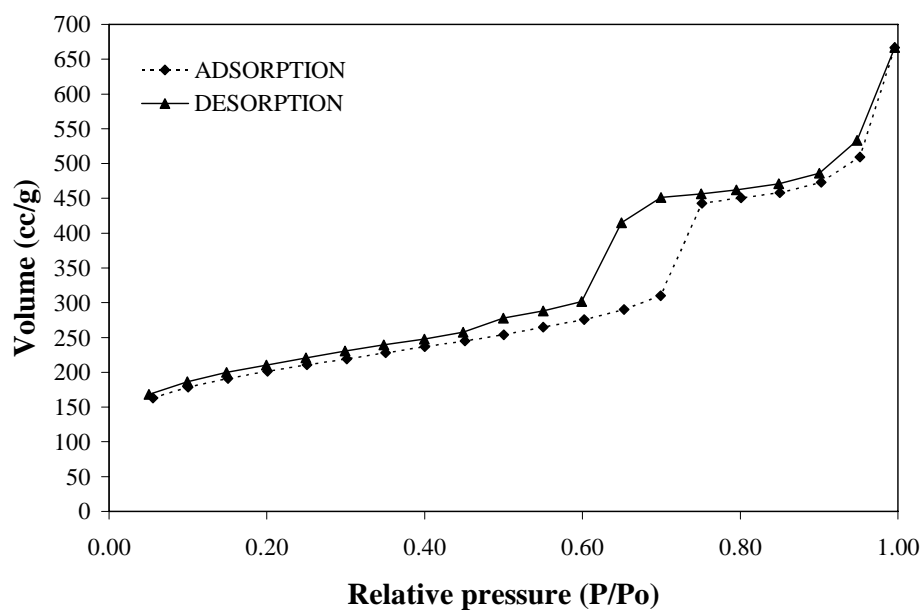
Appendix Figure B2 Sorption isotherm of SBA-15 product at hydrolysis-condensation temperature of 30°C and hydrothermal treatment temperature of 100°C



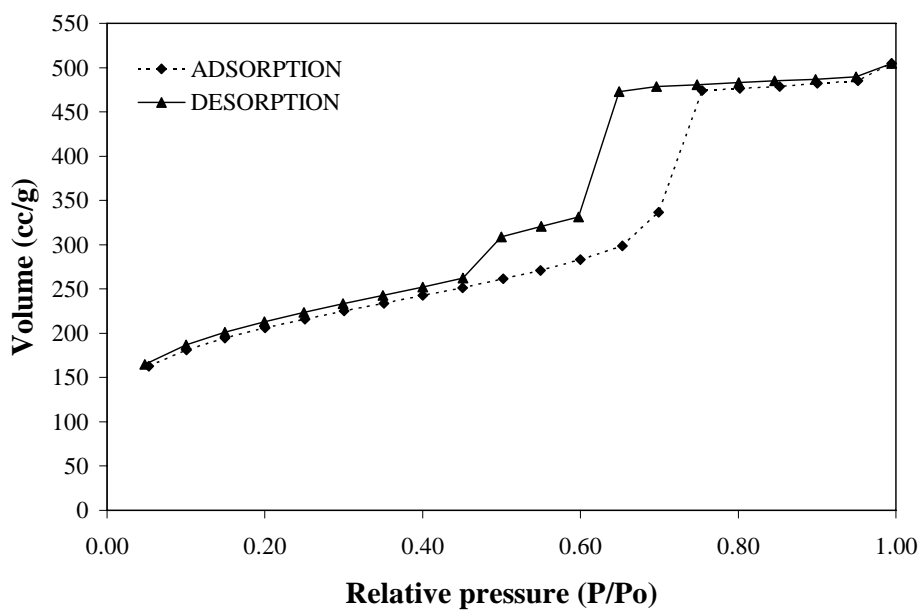
Appendix Figure B3 Sorption isotherm of SBA-15 product at hydrolysis-condensation temperature of 30°C and hydrothermal treatment temperature of 110°C



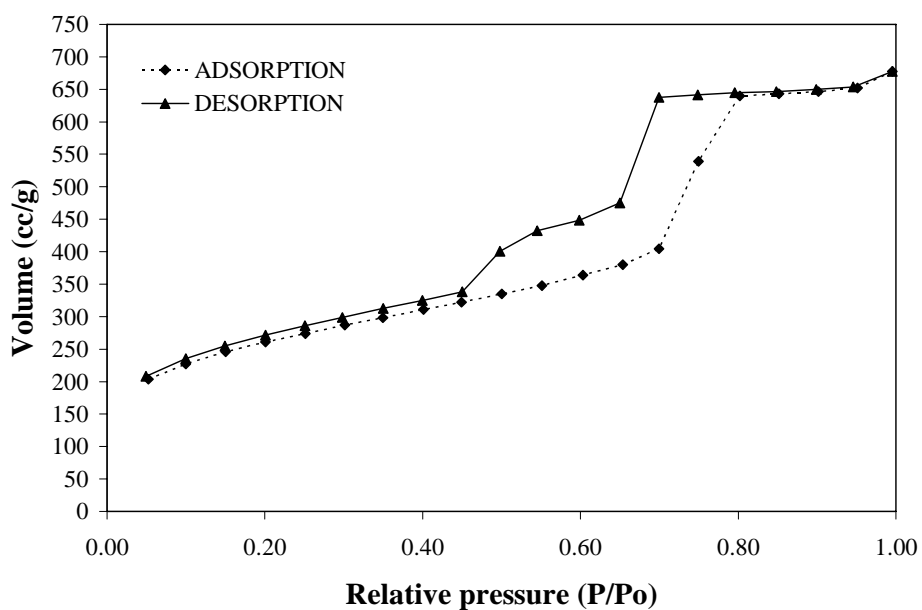
Appendix Figure B4 Sorption isotherm of SBA-15 product at hydrolysis-condensation temperature of 30°C and hydrothermal treatment temperature of 120°C



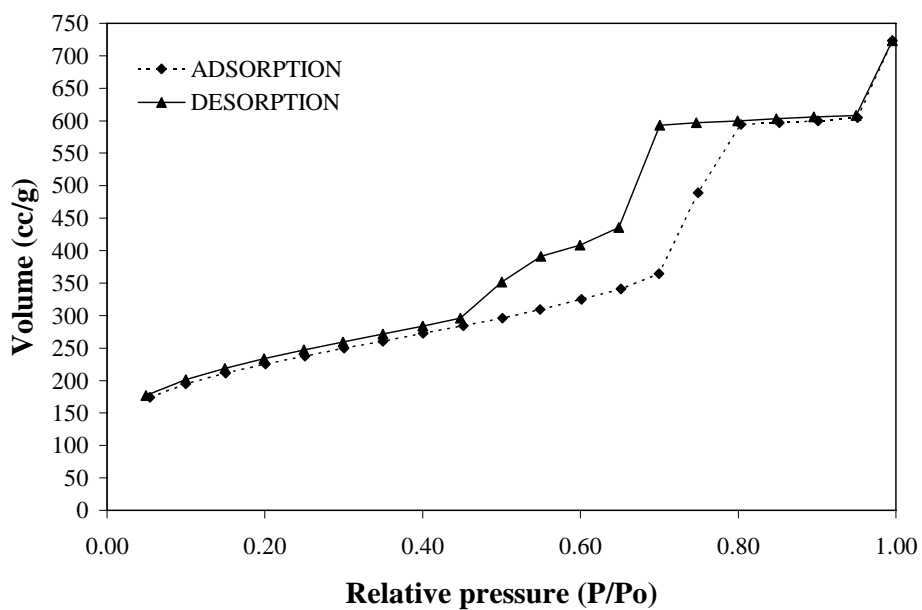
Appendix Figure B5 Sorption isotherm of SBA-15 product at hydrolysis-condensation temperature of 35°C and hydrothermal treatment temperature of 90°C



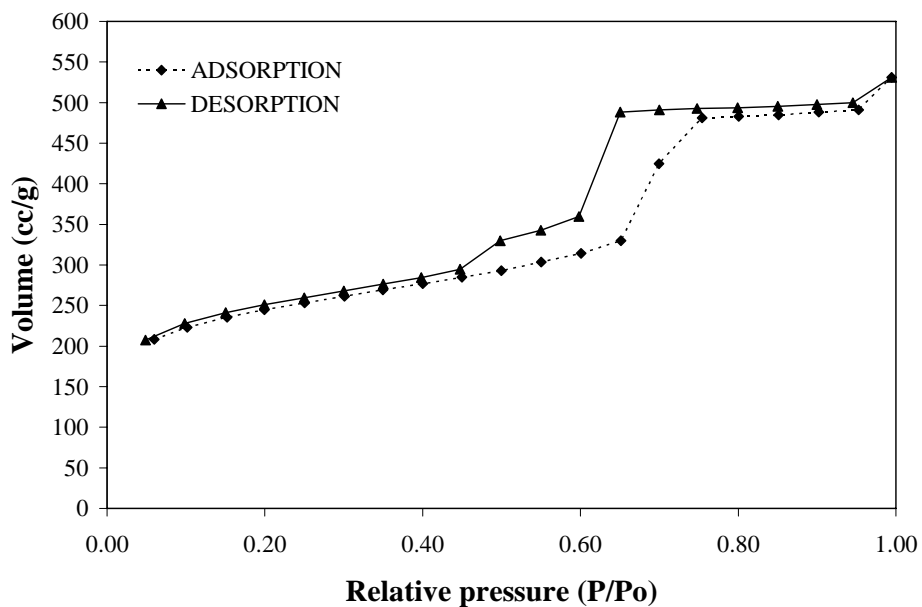
Appendix Figure B6 Sorption isotherm of SBA-15 product at hydrolysis-condensation temperature of 35°C and hydrothermal treatment temperature of 100°C



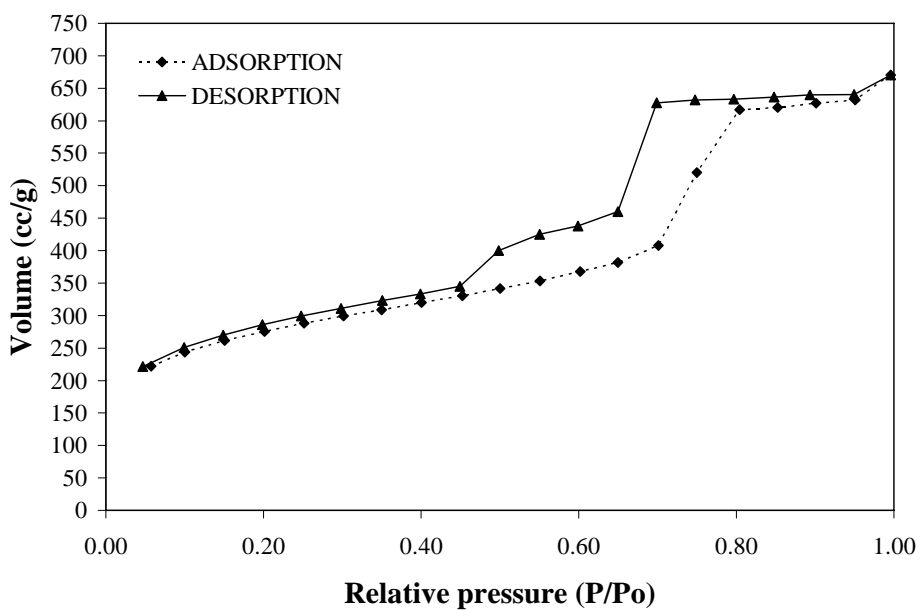
Appendix Figure B7 Sorption isotherm of SBA-15 product at hydrolysis-condensation temperature of 35°C and hydrothermal treatment temperature of 110°C



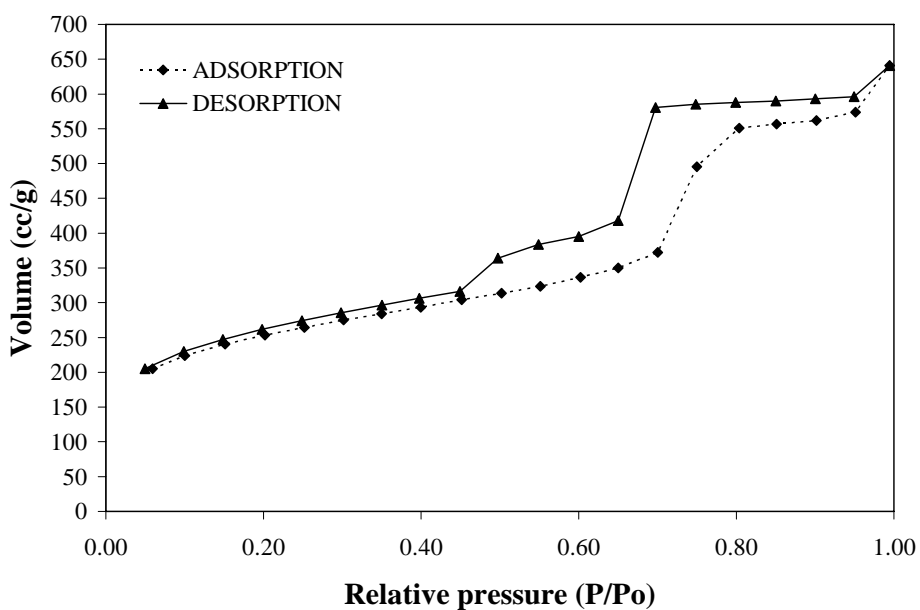
Appendix Figure B8 Sorption isotherm of SBA-15 product at hydrolysis-condensation temperature of 35°C and hydrothermal treatment temperature of 120°C



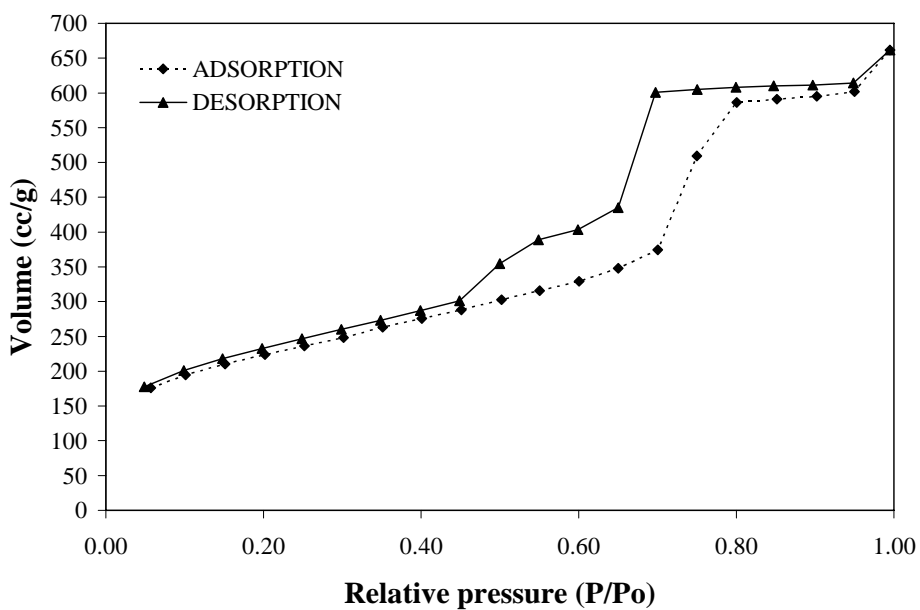
Appendix Figure B9 Sorption isotherm of SBA-15 product at hydrolysis-condensation temperature of 40°C and hydrothermal treatment temperature of 90°C



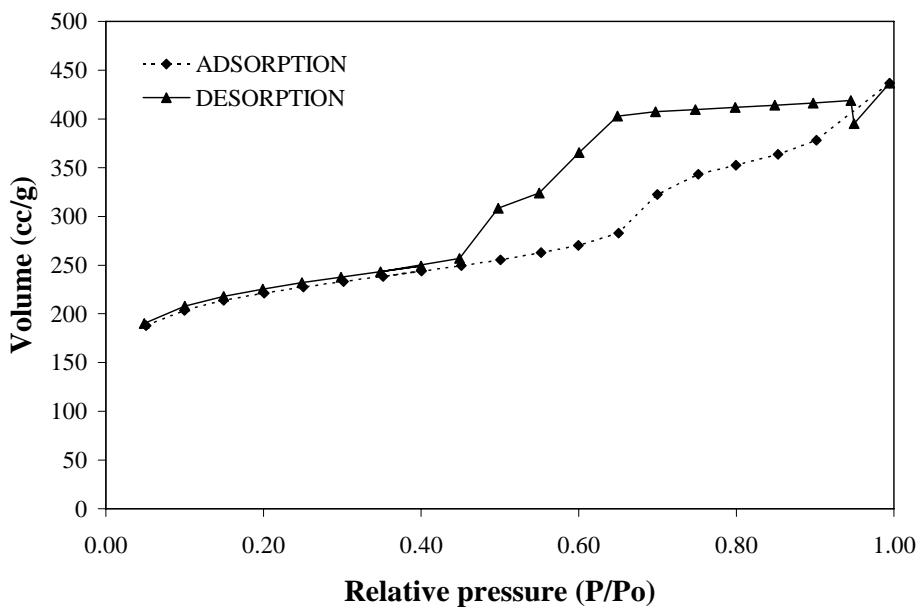
Appendix Figure B10 Sorption isotherm of SBA-15 product at hydrolysis-condensation temperature of 40°C and hydrothermal treatment temperature of 100°C



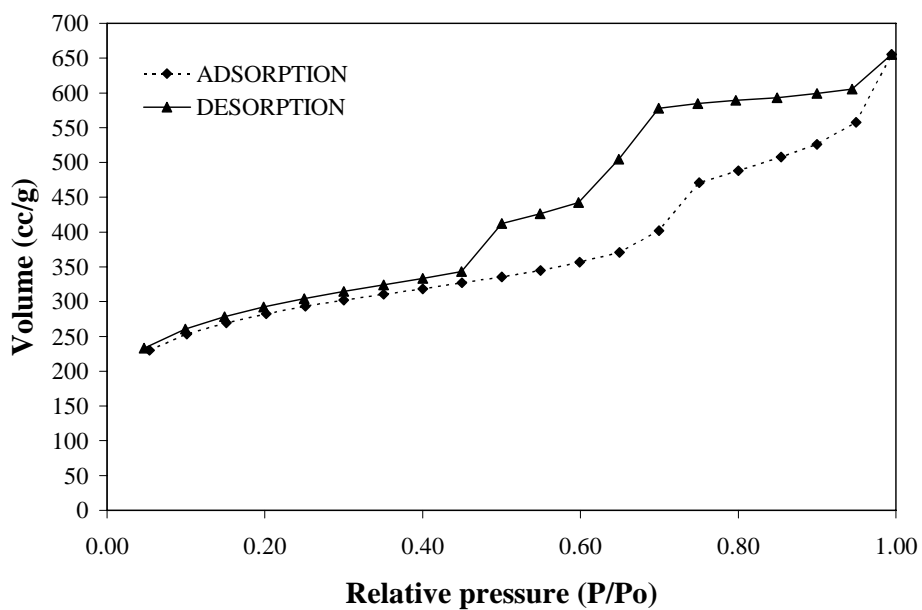
Appendix Figure B11 Sorption isotherm of SBA-15 product at hydrolysis-condensation temperature of 40°C and hydrothermal treatment temperature of 110°C



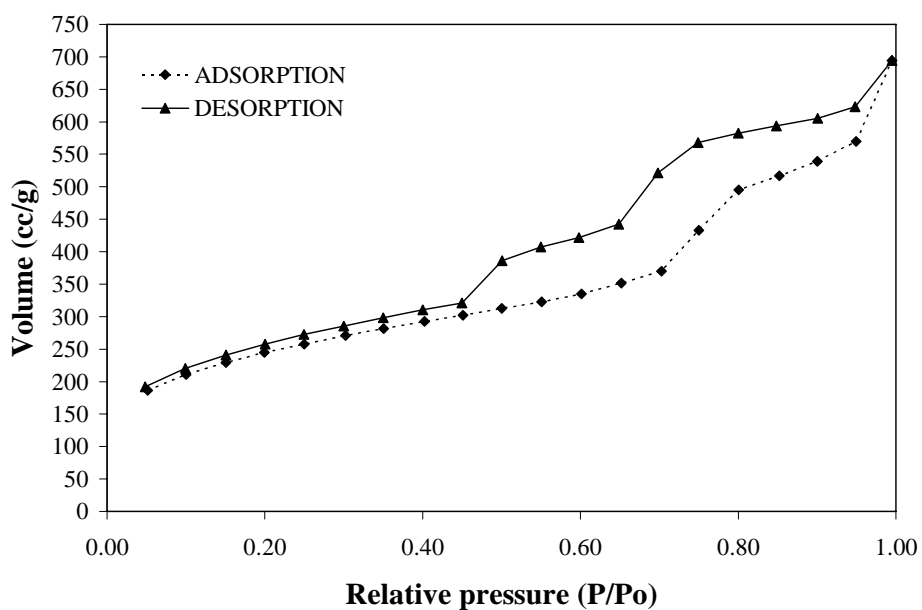
Appendix Figure B12 Sorption isotherm of SBA-15 product at hydrolysis-condensation temperature of 40°C and hydrothermal treatment temperature of 120°C



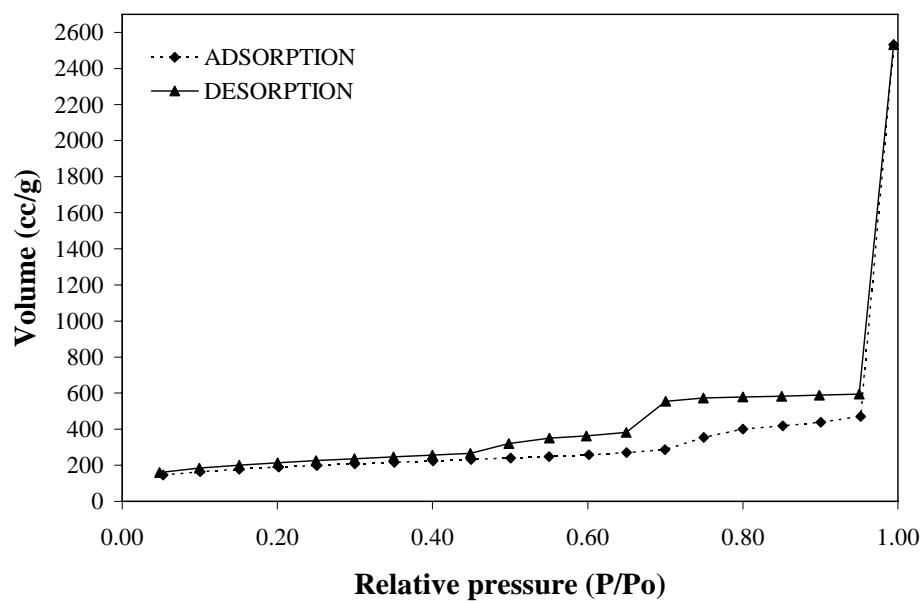
Appendix Figure B13 Sorption isotherm of SBA-15 product at hydrolysis-condensation temperature of 50°C and hydrothermal treatment temperature of 90°C



Appendix Figure B14 Sorption isotherm of SBA-15 product at hydrolysis-condensation temperature of 50°C and hydrothermal treatment temperature of 100°C



Appendix Figure B15 Sorption isotherm of SBA-15 product at hydrolysis-condensation temperature of 50°C and hydrothermal treatment temperature of 110°C



Appendix Figure B16 Sorption isotherm of SBA-15 product at hydrolysis-
condensation temperature of 50°C and hydrothermal treatment
temperature of 120°C

Appendix Table B1 Effect of synthesis temperature conditions on surface area, pore volume and pore size of SBA-15 products

Run No.	Synthesis temperature ¹ (°C)		Surface area (m ² /g)	Pore volume (cc/g)	Pore size (nm)
	Hydrolysis-condensation temp.	Hydrothermal treatment temp.			
1	30	90	669	0.25	6.5
2	30	100	631	0.22	7.7
3	30	110	797	0.28	7.7
4	30	120	636	0.22	7.7
5	30	90	673	0.25	6.5
6	30	100	694	0.25	7.7
7	30	110	885	0.31	7.7
8	30	120	773	0.27	7.7
9	50	90	794	0.32	6.5
10	50	100	919	0.34	7.7
11	50	110	844	0.4	7.7
12	50	120	766	0.27	7.7
13	50	90	708	0.29	6.5
14	50	100	927	0.36	7.7
15	50	110	839	0.29	7.7
16	50	120	647	0.25	7.7

¹ The molar ratio of 1 SiO₂ : 0.00875 Pluronic P123 : 200 H₂O : 4 HCl was used throughout in all experiment.

Appendix Table B2 Effect of swelling agents on SBA-15 properties

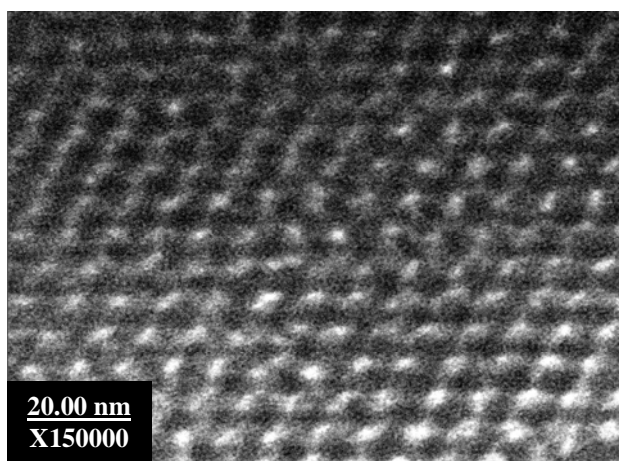
Swelling agents	Swelling agents/Pluronic P123 (g/g)	Pore size (nm)	Surface area (m ² /g)	Total pore volume (cc/g)	Run No. ¹
-	0	7.7	885	0.3	-
1,3,5-Trimethylbenzene	1	17.5	948	0.3	TMB 1
	2	17.5	991	0.35	TMB 2
	3	30.5	1703	0.6	TMB 3
	4	30.8	1188	0.4	TMB 4
2,3,4-Trimethylpentane	1	9.5	754	0.26	TPM 1
	2	11	723	0.25	TPM 2
	3	30	896	0.3	TPM 3
	4	30	1079	0.4	TPM 4
Tetrahexylammonium bromide	1	7.9	1156	0.4	THB 1
	2	4.3	987	0.3	THB 2
	3	4.9	896	0.3	THB 3
	4	4.9	346	0.1	THB 4
N,N - dimethyldecylamine	1	4.9	987	0.3	DMD1
	2	4.3	951	0.3	DMD 2
	3	4.9	1002	0.3	DMD 3
	4	4.9	978	0.3	DMD 4

¹ In all experiment; the molar ratios of 1 SiO₂ : 0.00875 Pluronic P123: 4 HCl : 200 H₂O under hydrolysis-condensation temperature at 35°C for 24 h and hydrothermal treatment temperature at 110°C for 24 h

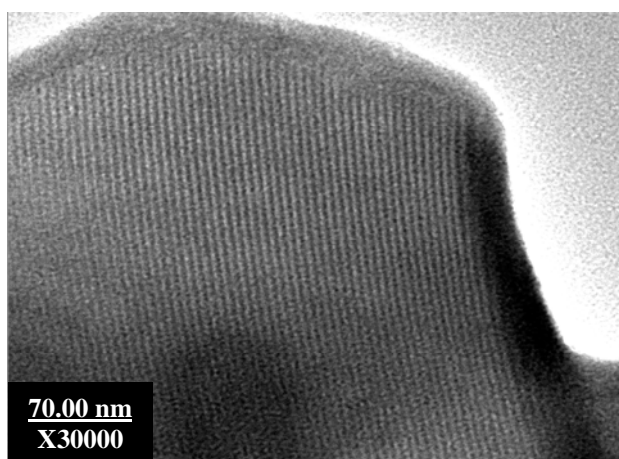
Appendix C

Transmission Electron Microscopy (TEM)

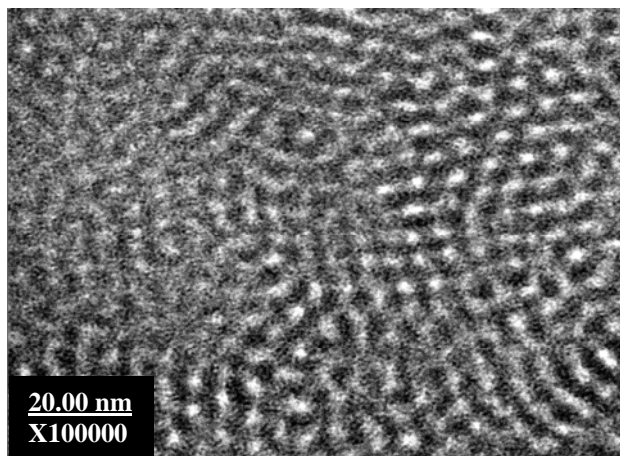
In all experiment, the third section of this research was analyzed by TEM in order to consider ordered pore structure of SBA-15 mesoporous silica. SBA-15 products prepared from the hydrolysis-condensation and hydrothermal treatment temperatures of (30-110 °C), (35-110 °C), (40-110 °C), (35-90 °C) and (35-100 °C) show narrow pore size distribution which were selected for analyzing TEM.



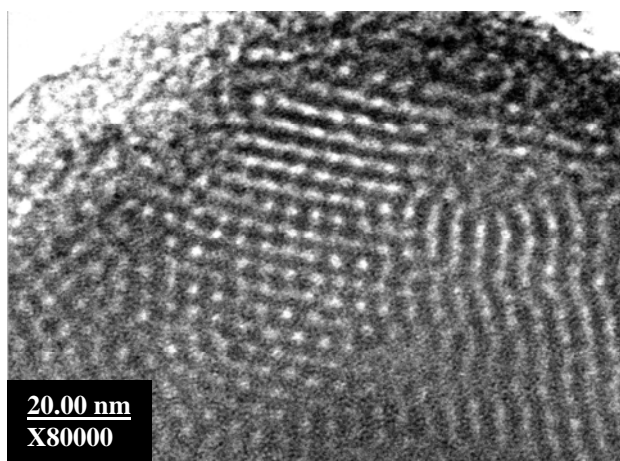
Appendix Figure C1 TEM image of SBA-15 mesoporous silica obtained from the hydrolysis-condensation temperature of 30°C and hydrothermal treatment temperature of 110°C



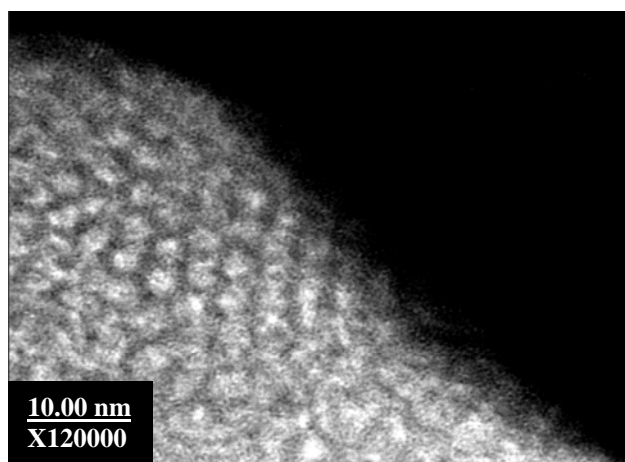
Appendix Figure C2 TEM image of SBA-15 mesoporous silica obtained from the hydrolysis-condensation temperature of 35°C and hydrothermal treatment temperature of 110°C



Appendix Figure C3 TEM image of SBA-15 mesoporous silica obtained from the hydrolysis-condensation temperature of 40°C and hydrothermal treatment temperature of 110°C



Appendix Figure C4 TEM image of SBA-15 mesoporous silica obtained from the hydrolysis-condensation temperature of 35°C and hydrothermal treatment temperature of 90°C



Appendix Figure C5 TEM image of SBA-15 mesoporous silica obtained from the hydrolysis-condensation temperature of 35°C and hydrothermal treatment temperature of 100°C

CURRICULUM VITAE

NAME: Miss. Suchada Issaraporn

BIRTH DATE: December 21, 1980

BIRTH PLACE: Chiangrai, Thailand

EDUCATION:	<u>YEAR</u>	<u>INSTITUTION</u>	<u>DEGREE/DIPLOMA</u>
	2004	KMIT'NB	B. SC. (IC)

SCHOLARSHIP/AWARDS:

Teacher assistant from ADB project of the Department of Chemical Engineering and Graduate School, Kasetsart University.